ISAS - INTERNATIONAL SCHOOL FOR ADVANCED STUDIES

Strongly Disordered Systems: from Polymer Statistics to Phase Transitions

Thesis submitted for the degree of
"Doctor Philosophiæ"

CANDIDATE

Paolo De Los Rios

SUPERVISOR

Prof. Amos Maritan

October 1996

SISSA - SCUOLA INTERNAZIONALE SUPERIORE DI STUDI AVANZATI
TRIESTE
Strada Costiera 11

TRIESTE

Table of Contents

List of Figures

List of Tables

1 Introduction to disordered systems

An important theme that emerged in many areas of current interest in condensed matter physics is the effect of randomness and disorder. Prior to the 1960s disorder and impurities were mostly considered as unavoidable hazes blurring the true behavior of ideal systems. In recent years, after a twist of mind, we learned that disorder itself can bring new unexpected and fascinating effects in condensed matter, such as the Anderson localization, the Kondo effect and the properties of glasses.

As it always happens, physicists tried to find paradigms and model systems in this new area of research. Their aim was to find the simplest way to add disorder to well known systems, with the hope to figure out the true effects of disorder.

In statistical mechanics one of the first models that was chosen was the Ising model. One of the main variations on the Ising theme are disordered ferromagnets, with exchange couplings taken according to some probability distribution symmetrical around zero. Due to strong frustration effects it is impossible for these models to build long range magnetic order (frustration just means that not all the interactions are satisfied by the corresponding spin configuration). Their feature to be in a magnetically "amorphous" state gained them the name of spin-glasses. These glasses are among the most studied disordered systems. Their behavior has been investigated with very many different techniques, ranging from renormalization group to mean-field (infinite range) to numerical. After more than twenty years of intensive research some of the basic issues are still unresolved, as we will see in Chapter 2. Moreover different and often successful approaches such as the mean-field and the droplet ones yield incompatible results, thus raising the question on whether any unifying picture exists at all.

More recently new problems arose that became as paradigmatic as spin-glasses, such as polymers in a disordered environment, and phase transitions in disordered media. Although they are unrelated problems, nonetheless they benefitted from the wisdom that the scientific community gained working on spin-glasses. It is not surprising therefore to learn that tools

such as replicas have been widely used on polymer problems, and that the droplet picture led to the very successful Imry-Ma argument for the random field Ising model and the Berker argument for the effects of disorder on first order phase transitions.

Polymers in disordered media form an extremely simple system as far as the description of their basic ingredients is involved. A polymer can be easily modeled with a self-avoiding walk (SAW), that is, a random walk with the simple property that it is not allowed to cross itself, with an energy which depends on the visited sites.. With an energy independent on the position, the properties of SAW's are well known both analytically (in two dimensions) and numerically. The addition of some disorder on the energies it can pick up from the space it is embedded in changes dramatically the behavior of the polymer. As we will show, finding even the simplest properties of this system goes far beyond the actual techniques of direct analysis. In order to extract as much information as possible we must resort to a more flexible approach, where mappings to other systems not only reveal deeper and richer interconnections between completely different problems, but also translate the original problem in languages that could be more suited to analytical solutions. Of course each problem benefits from the knowledge we have of the other. We at last discover that when there is just a "little bit" of disorder the behavior of the polymer is linked in an almost magic way to surface growth problems and to domain walls in two dimensional ferromagnets. Increasing the amount and the intensity of disorder, we will see that polymers are "percolating" through the lattice, and we will be able also to show that percolation is a relevant issue for polymer physics, especially from an algorithmic point of view. In particular invasion percolation, an extremal version of percolation, will prove of great conceptual usefulness to introduce another kind of disordered systems, that began to be studied in the late 1980s: self-organized extremal models.

The concept of scaling and of long-range correlations is not a new one in statistical mechanics since the description and comprehension of second order phase transitions. Yet, in equilibrium systems the lack of scale appears only for particular choices of the parameters that enter the description of the system. It has been recently realized instead that in Nature the lack of scale appears spontaneously in a great number of phenomena and structures such as the geometry of coast lines and river networks, the distribution of the magnitude of earthquakes and the distribution of mass extinctions in evolution. Of course it is very difficult to believe that all this phenomena are critical because by some chance the universe is just at the critical point for all of them; therefore we convince ourselves that behind them there should be some principle, hidden in the very dynamics of these systems, driving them in a state where there are long range space and time correlations. Systems as such are said to *self-organize* in a critical state. Because of its simplicity and its very loose relation with biology (and we are led to this choice by our personal interests) we will deal with a self-organized model of biological evolution that has been recently proposed.

Last, we will try to convince the reader that changing the probability of disorder for certain classes of systems can introduce new topological (mainly percolative) effects, where the usual arguments should be used with some care. In particular, against the insight provided us by the Imry-Ma and Berker arguments, some kind of phase transitions can be robust even in the presence of disorder. To show that this is the case we will address the problem of phase transitions in ^{3}He-^{4}He mixtures: these systems show rich phase diagrams, with both first and second order transitions, and tricritical points. Our approach on the Bethe lattice is handy enough to unveil the different features of the phase diagrams, thus climbing back to the roots of the topological effects introduced by disorder.

We hope that the reader who will make his/her trip to the end of this thesis will have the feeling that the multiform variety of techniques and arguments that can be used when dealing with disordered systems is what makes this area of research so exciting. The seeming impossibility to build up a set of only a few powerful and reliable tools to deal with disorder has to be seen as a richness much more than as something discouraging the researcher.

Actually, if we are flexible enough to use different approaches, from the most sophisticated analytical tools such as renormalization-group and replicas to non less trivial numerical ones such as cellular automata and Monte Carlo techniques, there is still plenty of space for exciting discoveries waiting around the corner.

2 Polymers in a Disordered Environment

Polymers raised in the years as one of the simplest systems where the effects of disorder is easier to understand while keeping all the main features of more complicated systems. They are easy to describe and numerical and analytical techniques are quite well developed when disorder is absent. Therefore most of their properties in the pure case are known. Any new features emerging in the presence of disorder can thus be safely attributed to the latter.

Henceforth it is not surprising to discover that in the last decade a great part of the statistical mechanics community looked at polymers in the hope to shed more light on the properties of disordered systems. It has been discovered that disordered polymers show many of the properties of other disordered systems, such as different regimes changing the strength of disorder and glassiness.

Among the nice properties they exhibited, they turned out to be enough stable against small variations of the distribution of disorder so that universality classes are well defined, but sensible enough that different universality classes emerged depending on the distribution of disorder.

Moreover, many other systems, as different as growing surfaces and percolation, are connected with some kind of polymer problem.

Polymers in disordered environment have thus been accepted as one of the paradigms of contemporary statistical mechanics.

After a review of the known results, in this chapter we will see that a clever use of the distribution of disorder can give elegant and sometime intuitive answers to many problems of current interest, such as finding the upper critical dimension for surface growth problems or getting the insight in the effects of the topological properties of disorder itself.

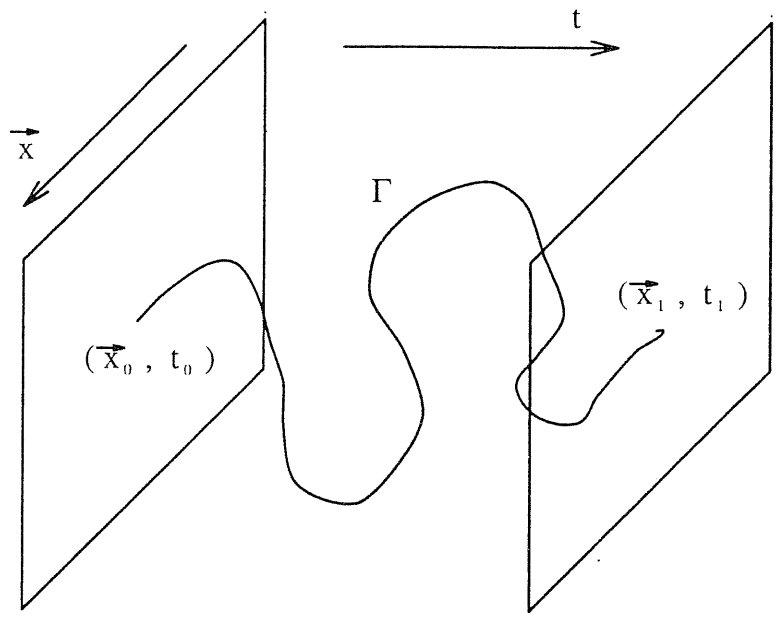

Figure 2.1: Coordinate setup for polymers in $D + 1 = d$ dimensions

2.1 The weak disorder universality class

The first model which has been extensively studied is the polymer on a landscape of energies taken from a probability distribution which is narrow around its mean value, such as a Gaussian.

Before proceeding further, it is useful to establish once for all a working setup. The polymer is a 1-dimensional object embedded in a d-dimensional space. For convenience the d dimensions are divided in D *space* ($\vec{x}$) and one *time* (t) dimensions. We will consider polymers with fixed extrema $(\vec{x}_0 = 0, t_0 = 0)$,$(\vec{x}, t)$, with the assumption that the boundary conditions will not be relevant in the thermodynamic limit (Fig. 2.1). Since the polymer is a one dimensional object its path Γ can be described by means of a real parameter $s \in [0, 1]$, $(\vec{x}(s), t(s))$.

The energy of the polymer depends on its configuration Γ. Assigning an energy density $\epsilon(\vec{x}, t)$ per unit length to every point, the energy of the polymer can be written as

$$E = \int_0^1 \epsilon(\vec{x}(s'), t(s'))\sqrt{|\dot{\vec{x}}(s')|^2 + \dot{t}^2(s')}ds' \tag{2.1}$$

where dots indicate derivatives with respect to the parameter s. The $\sqrt{|\dot{\vec{x}}|^2 + \dot{t}^2}ds$ term is the infinitesimal arc length of the curve Γ.

The quantity of interest is lowest energy path (ground state) Γ_{GS} on the energy landscape. Of course the specific conformation of the polymer and its ground state energy depend on the given realization of disorder, yet they show scaling features that instead are independent

of the very details of the system; therefore they can be considered as characterizing the universality class of the model.

The above mentioned quantities showing scaling behavior are the wandering of the polymer around its average $\vec{x}$ position and the fluctuations of its ground state energy.

The energy is an extensive quantity with respect to the length of the polymer, therefore we expect

$$E \sim L, \tag{2.2}$$

where

$$L = \int_0^1 \sqrt{|\dot{\vec{x}}(s')|^2 + \dot{t}^2(s')} ds', \tag{2.3}$$

is the length of the polymer. The length of the polymer scales with respect to the *time* distance between the extrema as

$$L \sim t^{D_f} \tag{2.4}$$

where D_f is the fractal dimension of the polymer. The energy is an extensive quantity, and we therefore expect

$$E \sim L \sim t^{D_f}. \tag{2.5}$$

It is now due time for some intuitive considerations. Any polymer with a fractal dimension $D_f > 1$ will have an energy increasing more rapidly than its duration t. Since we are looking for the ground state, the polymer will try to minimize its energy: the energy of a fractal polymer ($D_f > 1$) grows much faster than that of a linear one ($D_f = 1$), so that fractal configurations are not favorable, and $D_f = 1$. In this case the polymer is said to be a *self-affine* structure. Some simple topological consequences follow. A fractal object is characterized by the same geometric features on any length scale. In particular, in order to have a length content which grows faster than the sample dimensions, the polymer will wander back and forth many times in the time direction. On the contrary, a non fractal polymer ($D_f = 1$) will only occasionally have such behavior: on longer and longer length scales a *linear* polymer is *directed*; this means that the $\vec{x}$ coordinate is a one-valued function of the time coordinate (this of course does not rule out completely overhanging configurations on the microscopic scale; yet, they will be very rare). Therefore in what follows we will drop the heavy s-parametrization of the polymer, and use more simply $\vec{x}(t)$. Eq.(2.1) becomes therefore

$$E(t) = \int_0^t \epsilon(\vec{x}(t'), t') \sqrt{1 + |\partial_{t'} \vec{x}(t')|^2} dt' \tag{2.6}$$

Fluctuations of the ground state energy are intrinsically defined over many different realizations: given a disorder realization, the ground state energy is uniquely and precisely defined, free of fluctuations. Therefore we first define the average ground state energy

$\overline{E_{GS}}$ (from now on overbars will indicate averages over many different realizations of the disorder), and the energy fluctuations are

$$\Delta E = \sqrt{\overline{E_{GS}^2} - \overline{E_{GS}}^2}. \tag{2.7}$$

Energy fluctuations show non trivial scaling behavior with an exponent ω

$$\Delta E \sim t^{\omega}. \tag{2.8}$$

The other characterizing quantity is the scaling exponent of the wandering of the polymer around its average position.

The average $\vec{x}$ position of the polymer is

$$< \vec{x} >= \frac{1}{L}\int_0^t \vec{x}(t)dt, \tag{2.9}$$

where the angular brakets indicate sample averages, that is averages taken on a specific realization of disorder.

Since the distribution of disorder is isotropic and homogeneous over the D-dimensional space, there will be no preferential direction for the polymer. Therefore an intuitive expectation is $< \vec{x} > \to 0$ in the thermodynamic limit. This result can be easily verified numerically. Actually, as already pointed out, when dealing with quenched disordered systems also the average over different disorder realizations must be taken. Due to symmetry considerations,

$$\overline{< \vec{x} >} = 0 \tag{2.10}$$

independent of the size of the system. This is a first example of a self-averaging (even if trivial) quantity: the average over just one realization of disorder is, in the thermodynamic limit, equal to the average over many realization.

The wandering W of the polymer around its average position (which, for what has been stated before, is the origin) can therefore be expressed as

$$W^2(t) =< |\vec{x}|^2 >= \frac{1}{L}\int_0^t |\vec{x}(t')|^2 dt'. \tag{2.11}$$

This quantity also shows non trivial scaling behavior with respect to the distance between the extrema. Precisely, one can define a wandering exponent ζ through the scaling of $W(t)$ as

$$W(t) \sim t^{\zeta} \tag{2.12}$$

Again we are dealing with a self-averaging quantity; in fact also $\overline{W(t)} \sim t^{\zeta}$.

It is still possible to argue some properties of ζ on the basis of simple *a priori* considerations. The wandering of the polymer is a measure of its transverse displacement. Therefore

a rough but instructive estimate of the length of the polymer can be obtained from the expression

$$L = \sqrt{L_{||}^2 + L_{\perp}^2} = \sqrt{t^2 + t^{2\zeta}}. \tag{2.13}$$

We already stated that $L \sim t$; therefore the second term $t^{2\zeta}$ must be subleading and $\zeta \leq 1$.

As in usual critical phenomena, there are relations among the exponents. Let us take again the expression (2.6). The random energy density can be expressed as

$$\epsilon = \epsilon_0 + \eta \tag{2.14}$$

where ϵ_0 is the average energy density, and η is a new random variable with the same distribution as ϵ around 0. In the hypothesis of directed self-affine polymers with $\zeta < 1$ (the possibility of $\zeta = 1$ is left apart for the moment, and *a posteriori* verified), the length element can be approximated because the polymer has little fluctuations around the origin, and $|\partial_t \vec{x}| \ll 1$

$$\sqrt{1 + |\partial_t \vec{x}|^2} \sim 1 + \frac{1}{2}|\partial_t \vec{x}|^2 \ . \tag{2.15}$$

The energy can therefore be approximated as

$$E = \epsilon_0 L_{||} + \int_0^t \frac{1}{2}\epsilon_0 |\partial_{t'} \vec{x}(t')|^2 dt' + \int_0^t \eta(\vec{x}(t'), t') dt' \tag{2.16}$$

where terms such as $\eta\, |\partial_t \vec{x}|^2$ and of higher order have been neglected. The first term in the *r.h.s.*, of (2.16) ensures the extensivity of the energy, and we already discussed about it. Forgetting about it we do not loose any generality. The second term in the *r.h.s.* of (2.16) represents the fluctuations around the mean value of the energy and it provides the relation between the exponents we are looking for. In fact it should scale as t^{ω}. On the other hand the $|\partial_t \vec{x}(t)|$ term in the integral accounts for the infinitesimal transverse wandering of the polymer; therefore, as already pointed out, it will scale as $t^{\zeta - 1}$, and the overall term in the integral will scale as $t^{2\zeta - 1}$; the relation between the exponents is at last

$$\omega = 2\zeta - 1. \tag{2.17}$$

As simple as it seems, the problem of polymers in weak disorder has proven almost as subtle and difficult to attack as the more celebrated spin-glass problem. We will try to give a short review of the exact results that are known up to date, and of some of the most fruitful methods of investigation that have accumulated in the years. All this wisdom will prove unvaluable for our work.

2.2 The two dimensional problem: connections with other models and exact solutions

In traditional statistical mechanics people got recently used to think that two dimensional systems are somewhat privileged. Most known exact solutions actually are given in two dimensions, using tools such as Conformal Invariance. Yet it is a good exercise of humility to recognise that there are two dimensional systems that are quite elusive and resistent to all the known approaches. Just to mention two of them, no exact results are known for directed percolation and for branched polymers. Disordered systems are even more difficult to tackle, and their properties more uncertain and subject to periodical debates. Nonetheless the properties of the ground state of polymers in a two dimensional weakly disordered landscape of energies revealed so rich of connections to other problems that a plethora of methods has been devised to extract as much information as possible from them. In particular two techniques proved very powerful, providing the exact values of the exponents ω and ζ. Both of them also gave us a deep insight in the physics of the problem.

2.2.1 Mapping to the Kardar-Parisi-Zhang equation of surface growth

Let us consider again the expression of the energy of the polymer,

$$E = \int_0^t \left[\frac{1}{2}\epsilon_0 |\partial_t' \vec{x}(t')|^2 + \eta(\vec{x}(t'), t')\right] dt' \tag{2.18}$$

We can write a partition function for the polymer at finite temperature T, that, after a rescaling of ϵ_0 and of the noise strength, can be taken equal to

$$Z(\vec{x}, t) = \int_{(0,0)}^{(\vec{x},t)} d[\vec{x}] e^{-\int_0^t \left[\frac{1}{2}\epsilon_0 |\partial_t' \vec{x}(t')|^2 + \eta(\vec{x}(t'),t')\right] dt'} \tag{2.19}$$

This expression is susceptible of an imaginary time path integral interpretation, and the corresponding Schroedinger equation is

$$\dot{Z} = \epsilon_0 \nabla^2 Z + \eta(\vec{x}, t) Z \tag{2.20}$$

Starting from this equation we begin to build the bridge toward other problems, thus discovering other members of the universality class of polymers in weak disorder. By this means we will also find the exact values of the exponents ζ and ω in $d = 1 + 1$ dimensions. First, we can perform a change of variable, the so called Cole-Hopf transformation

$$Z(\vec{x}, t) = e^{\frac{\lambda}{2\epsilon_0} h(\vec{x}, t)} \tag{2.21}$$

The variable h clearly plays a role similar to the free-energy of the problem; with this new variable, Eq.(2.20) becomes

$$\partial_t h = \epsilon_0 \nabla^2 h + \frac{\lambda}{2} (\nabla h)^2 + \frac{2\epsilon_0}{\lambda} \eta \tag{2.22}$$

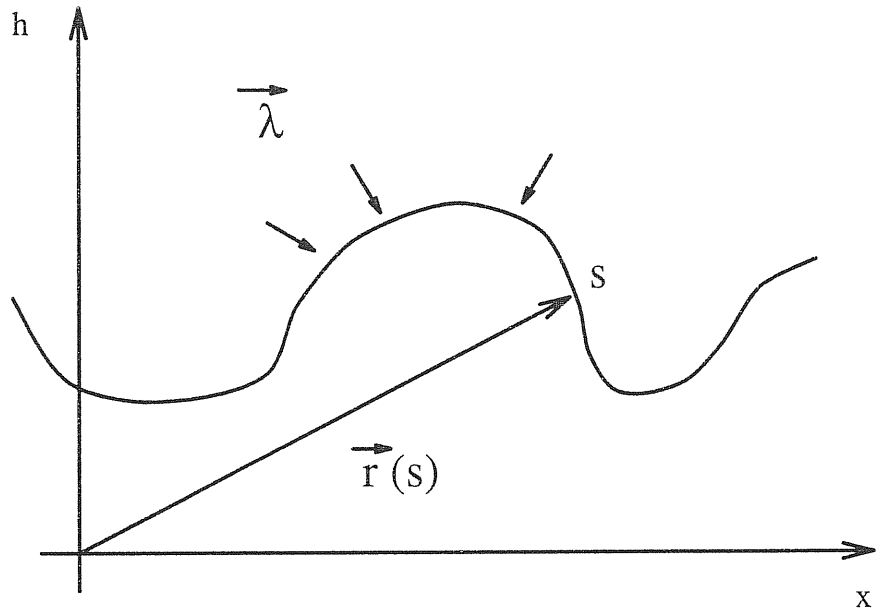

Figure 2.2: Surface growing under a flux J

This equation is the Kardar-Parisi-Zhang (KPZ) equation describing the growth of a surface of height h under the influence of an external flux of particles (actually Eq.(2.22) is written in a frame comoving with the surface). The $\nabla^2 h$ term in the *r.h.s* of (2.22) accounts for surface relaxation, whereas the non linear term comes from lateral growth. A very simple and instructive way to derive the non-linear term makes use of a Reparametrization Invariance (RP) formulation of the problem. The basic idea of RP is both profound and simple: the properties and features of the growth of the surface must be independent on the way we parametrize it. Under a flux of particles sticking along the local normal to the surface as in Fig.2.2. the surface grows according to the equation

$$\dot{\vec{r}}(s) = \lambda \hat{n}(s) \tag{2.23}$$

To obtain (2.22) we assume that the surface is a single-valued function of the sample x coordinate (there are no overhanging configurations). If this is the case, then we can parametrize the surface as $\vec{r}(x,t)$. Written at length the full equation (2.23) is now

$$\begin{pmatrix} \dot{x} \\ \dot{h} \end{pmatrix} = \begin{pmatrix} \frac{-\partial_x h}{\sqrt{1+(\partial_x h)^2}} \\ \frac{1.0}{\sqrt{1+(\partial_x h)^2}} \end{pmatrix}. \tag{2.24}$$

Then we write the total time derivative $\dot{h}$ as

$$\dot{h} = \partial_t h + \partial_x h \, \dot{x}. \tag{2.25}$$

Substituting in (2.23) and taking the small gradients approximation ($|\partial_x h| \ll 1$) we obtain the non-linear term in (2.22).

The Cole-Hopf transformation (2.21) teaches us that the fluctuations of the height of the surface are related to the fluctuations of the energy of the polymer.

The fluctuations of the surface have a power law behavior in time and in space; the roughness of the surface has a time behavior dictated by the scaling law

$$W(L,t) \sim t^{\beta} f(\frac{t}{L^z}), \tag{2.26}$$

where L is the length of the sample; the scaling function $f(x)$ is such that

$$f(x) = \begin{cases} const & x \ll 1 \\ x^{-\beta} & x \gg 1 \end{cases} \tag{2.27}$$

Therefore we can identify two different regimes; for small times ($x \ll 1$ in (2.27)) the roughness grows with a power law in time characterized by an exponent β; then there is a crossover to a different regime, where the roughness grows with a power law of the length of the sample characterized by an exponent $\alpha = \beta z$. The exponent z is the *dynamical exponent* of the system, and it rules the behavior of the crossover time. From a renormalization group point of view it tells what is the characteristic exponent with which we must rescale the time when we rescale the length in order to see the same behavior.

As for the polymer problem, the exponents we just defined are related to each other. Schematically, we substitute

$$h \sim L^{\alpha} \quad t \sim L^{z} \tag{2.28}$$

in (2.22). Since we want the non-linearity to be relevant, we ask that it scales as the time derivative in the *l.h.s.* of (2.22). The relation

$$\alpha + z = 2 \tag{2.29}$$

follows.

Now we can write down a bridge between polymers and surface growth. As we pointed out the fluctuations with time of the surface height correspond to the fluctuations with length of the polymer energy, and therefore we have $\omega = \beta$. The dynamical exponent of surface growth relates the length of the sample (which corresponds to the $\vec{x}$ polymer coordinate) to time. Again we find a correspondence between exponents: $\zeta = \frac{1}{z}$. Consequently relation (2.29) becomes equal to (2.17).

The mapping to the KPZ equation allows us to determine the exponents for the 2d polymer. We can in fact write the Fokker-Plank equation corresponding to (2.22) as

$$\frac{\partial P[h;t]}{\partial t} = -\int d\vec{x} \frac{\delta}{\delta h} \left\{ \left[\epsilon_0 \nabla^2 h + \frac{\lambda}{2} (\nabla h)^2 \right] P \right\} + \int d\vec{x} \frac{\delta^2}{\delta h^2} P. \tag{2.30}$$

where $P[h;t]$ is the probability of a surface configuration $h(\vec{x})$ at time t. The above equation admits a time-independent (stationary) solution for $d = 1$; specifically

$$P[h] = \exp\left[-\frac{1}{2}\epsilon_0 \int_0^L dx(\nabla h)^2\right]. \tag{2.31}$$

Interestingly, this is the same solution as for the Fokker-Plank equation associated with the Edward-Wilkinson (EW) (Edwards and Wilkinson (1982)) equation

$$\partial_t h = \epsilon_0 \nabla^2 h + \eta, \tag{2.32}$$

which governs the dynamics of a surface under relaxation and noise. Eq. (2.32) can be easily solved since it is linear in h. However, much more easily, with the same scaling assumptions $h \sim L^\alpha$, $t \sim L^z$, as before we are able to obtain the values of the exponents for (2.32). In fact simply equating the scaling exponents of the *l.h.s.* and of the *r.h.s.* of (2.32) we obtain $z_{EW} = 2$, $\alpha_{EW} = \frac{2-D}{2}$ when $D \leq 2$, $\alpha = 0$ when $D > 2$. Solution (2.31) holds in the infinite time limit, when the relevant scaling of the roughness is $W \sim L^\alpha$. Therefore we find that, in $d = 1+1$, $\alpha_{KPZ} = \alpha_{EW} = \frac{1}{2}$. Using (2.29) we obtain $z = \frac{3}{2}$ and $\beta = \frac{1}{3}$. Going back to the polymer problem using the relations between the exponents we eventually find

$$\zeta = \frac{1}{z} = \frac{2}{3} \qquad \omega = \beta = \frac{1}{3} \tag{2.33}$$

This has been the first exact derivation of the exponents of the polymer in weak disorder.

Actually the mapping to the KPZ equation is very important and it is a conceptual achievement; in fact it shows that the concept itself of universality class in these problems has a different character with respect to the usual one in equilibrium statistical mechanics. We are used in fact to think that different systems share the same exponents for analogous quantities (*e.g.* order parameter, susceptibility, specific heat). In this case, instead, we clearly see that the quantities that are characterized by the same exponents have nothing in common from the physical point of view (surface height fluctuations in KPZ and energy fluctuations in polymers). Therefore the concept itself of universality class is more subtle in these cases, and there is no general recipe to establish it (as for example space dimensions, order parameter dimensions and symmetries in equilibrium statistical mechanics).

The family of systems sharing the same exponents of the two dimensional polymer in weak disorder and of the $1+1$ dimensional KPZ equation is actually still larger. It can be shown in fact that the universality class of directed polymers comprises also the Burgers equation, describing the motion of a randomly stirred fluid (Forster, Nelson and Stephen (1977)) and domain interfaces in dirty two dimensional ferromagnets (Huse and Henley (1985), Kardar (1985), Huse, Henley and Fisher (1985)).

A more direct approach to polymers aiming to the determination of the two dimensional exponents has been pursued using the replica trick (Kardar (1987)). The values $\zeta = \frac{2}{3}$ and

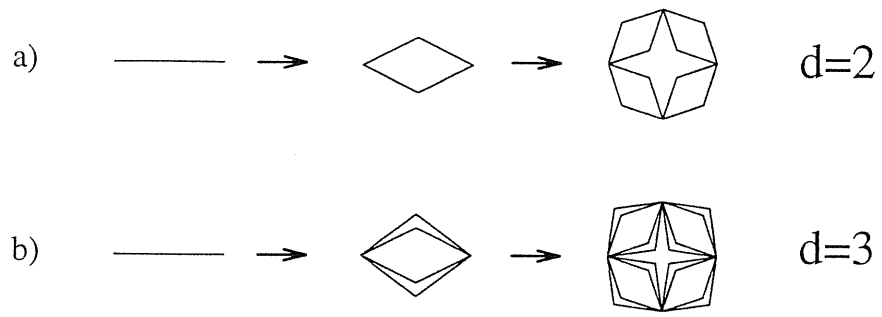

Figure 2.3: Hierarchical lattices considered in this paper and corresponding to (a) $d = 2$ and (b) $d = 3$.

$\omega = \frac{1}{3}$ are again obtained; moreover it has been found that the directed polymer problem is equivalent to a system of n bosons on a line interacting via attractive contact interactions, in the limit $n \to 0$ (of course this problem of interpretation is one of the prices we pay for the useful replica approach).

2.2.2 Renormalization group scheme on hierarchical lattices

A very nice renormalization group approach has been pursued by Derrida and Griffiths (Derrida and Griffiths (1989)) using *hierarchical lattices*. A hierarchical lattice is a fractal object that can be constructed recursively. The building block is the transformation from the single bond to a more articulated structure, as depicted in Fig. 2.3. Applying this transformation to each bond of the structure, we add more and more details to the lattice, just as if we were using stronger and stronger magnifying lenses to look at it. This process can be seen as a succession of *fine graining* steps. The basic transformation allows us also to compute the fractal dimension of the resulting lattice. In fact at every step the length of the lattice doubles and its bond content (its *volume*) is multiplied by the bond content of the more articulated structure. For example, Fig.2.3a has a fractal dimension $D_f = Log_{LengthMultiplicationFactor}(BondContent) = Log_2 4 = 2$, and Fig.2.3b has $D_f = 3$.

In the literature many of these lattices with different articulated (decorated) structures (see Fig.2.4) have been used for different purposes: the possibility of tuning the fractal dimension of the lattice is a far-reaching possibility to test the behavior of systems for non-integer dimensions and therefore study, for example, scaling laws involving the dimensions of the system.

As well as a fine graining step has been defined, we can also define its inverse, the *coarse graining* step, obtained reversing the arrows in Fig.2.3. Starting from the full (infinite) lattice, we begin to substitute the single bond to the decorated structure. The process stops when all the lattice has been transformed to a single bond. This procedure implements in a very natural way the real-space renormalization group scheme, that on these lattices

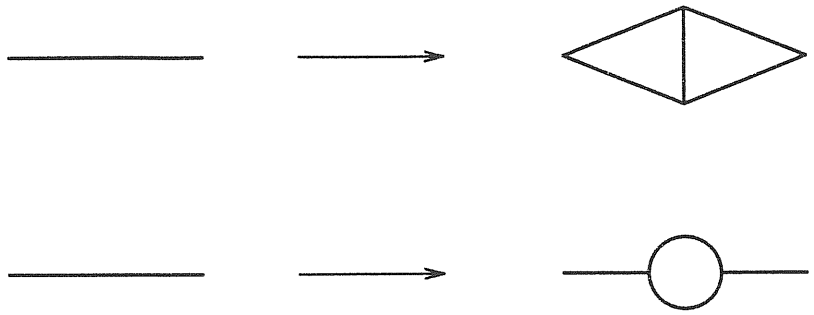

Figure 2.4: Hierarchical lattices considered in this paper and corresponding to (a) $d = 2$ and (b) $d = 3$.

becomes exact.

We assign to each bond of the lattice an energy E taken from a distribution $P_0(E)$. Then we must find the renormalized energy distribution for the single bond energy E' after the coarse graining transformation. For sake of simplicity we will focus on the $2D$ lattice in Fig.2.3a. Since we are looking for the probability distribution of the ground state energy, we must ensure that the energy is exactly E' on one of the two sides of the lattice and higher or equal on the other one. Therefore we define the probability that the energy of the polymer is E' on one side, $Q_0(E')$, as

$$Q_0(E') = \int P_0(E)P_0(E' - E)dE \tag{2.34}$$

where we did not specify the extrema of integration which are clearly dependent on the distribution of disorder $P_0(E)$. Next we define the coarse grained ground state energy distribution $P_1(E')$ as

$$P_1(E') = Q_0(E') \int_{E'} Q_0(E'')dE''. \tag{2.35}$$

The above recursion relation can then be iterated.

It is important to observe that the iteration of (2.35) does not have a fixed point, as can be argued from the extensivity of the energy: the ground state energy of the polymer is an extensive quantity with the size of the system or, which is the same, with the number of coarse graining steps we perform; therefore the mean value of the renormalized energy (2.35) grows from step to step. As a consequence, we do not look for any fixed point of the iteration, as in usual real-space renormalization schemes. Instead, we consider the behavior of the variance σ of the ground state energy probability distribution with the iterations. Since any iteration corresponds to a coarse graining step that reduces of a factor two the length of the lattice, we expect a power law behavior such as

$$\frac{\sigma_{n+1}}{\sigma_n} = 2^{\omega} \quad , \tag{2.36}$$

where ω has the same meaning as for the directed polymer problem described above. We

cannot define a wandering exponent ζ because the transverse metric properties of the hierarchical lattice are absent.

Derrida and Griffiths followed the recursion numerically starting with a bimodal distribution of energy $P_0(E)$,

$$P_0(E) = a_{-1}\delta(E+1) + a_1\delta(E-1) \tag{2.37}$$

taking care that the lowest energy did not percolate ($a_{-1} < p_c$). They obtained $\omega = 0.298....$ very close to the predicted theoretical value in two dimensions $\omega = \frac{1}{3}$.

Actually this discrepancy must not be intended as a breakdown of universality, because the hierarchical lattice of fractal dimension 2 is not a euclidean lattice: many of the connectivity and metric properties of euclidean lattices are lost. Nonetheless the striking result is that the value of ω on hierarchical lattices is very close to the one on euclidean lattices. This result gives to hierarchical lattices the full dignity of a very useful investigation tool.

In their paper Derrida and Griffiths also addressed an analytical solution using a $1+\epsilon$ expansion around the exact solution in 1 dimension. They found very good agreement with the numerical implementation of (2.35) generalized for arbitrary dimension and using (2.37). We address this problem in the Appendix 1, where we also give some hint of a possible extension.

At present we do not know of any analytic solution for this problem for the true two dimensional hierarchical lattice.

2.3 Polymers in strong disorder

As we already pointed out in the previous sections, the problem of directed polymers (DP) in random media (Kardar and Zhang (1987), Fisher and Huse (1991), Halpin-Healy and Zhang (1995)) has recently attracted much attention because of its possible connections with other systems, such as domain walls in random ferromagnets (Huse and Henley (1985), Kardar (1985), Huse et al. (1985)), interface growth (Kardar, Parisi and Zhang (1986)) and directed percolation (for a review see ref. (Barabasi and Stanley (1995))). In particular it is well known that the domain wall geometry in weakly disordered ferromagnets, the dynamics of growing interfaces governed by the Kardar-Parisi-Zhang (KPZ) (Kardar et al. (1986)) equation and DP in a weakly disordered landscape are related to each other in two dimensions via the Burgers equation (Barabasi and Stanley (1995), Forster et al. (1977)). However there are many physical systems where, in the considered length scales, the weak disorder approximation is not appropriate. This happens when physical features have a broad distribution and we will refer to this situation as the strong disorder case. Examples can be found in a variety of situations, including transport in amorphous semiconductors

at low temperatures, electrical conduction and fluid flow in porous rocks, and the magnetic properties of doped semiconductors. (Ambegaokar, Halperin and Langer (1971), Hirsch and Jose (1980), Dasgupta and Ma (1980), Bhat and Lee (1982), Fisher (1992), Katz and Thompson (1986), Berman, Orr, Jaeger and Goldman (1986)).

It has been shown that in this limit the self-affine domain walls become fractally rough with significant overhanging configurations, thus leading to a new universality class (Cieplak, Maritan and Banavar (1994)a, Cieplak, Maritan and Banavar (1994)b, Cieplak, Maritan, Swift, Bhattacharaya, Stella and Banavar (1995)).

The non directedness of the domain wall configurations in the strong disorder limit makes it clear that the weak disorder connection with DP is lost. Then the question arises about the behavior of DP in a strongly disordered landscape and about the influence of the constraint of directness on the universality class (Cieplak et al. (1994)a).

The directed optimal path problem is defined in a $d+1$ dimensional lattice, where a random energy ϵ_b is assigned to each bond and is independently distributed all over the lattice. The energy of a directed path $\wp$ (steps occur along bonds which have a positive projection on the $(1,1\ldots,1)$ direction) is defined as

$$E(\wp) = \sum_{b\in\wp} \epsilon_b \tag{2.38}$$

If the distribution is very broad, a useful approximation is to assume that the sum of variables from the distribution is simply equal to the largest one. Then the energy in eq.(2.38) becomes

$$E_m(\wp) = \max_{b\in\wp} \epsilon_b \tag{2.39}$$

It is now due to understand to what extent the used approximation (2.39) is valid. As we already mentioned in Subsec.2.2.2, when dealing with directed polymers in weak disorder the result obtained on hierarchical lattices is independent on the details of the energy probability distribution that is used as a starting point for the iteration (2.35). This can be seen as a consequence of the Central Limit Theorem (which states that any probability distribution with finite first and second moments would renormalize to a Gaussian distribution using (2.38)). Therefore we have to be very careful in the assumption of a *broad* energy distribution: broad distributions can be considered as such as long as the system is still not in thermodynamic limit. We can identify three length scale regimes: the microscopical length scale, where the energy probability distribution is just the one we choose to assign energies to the bonds; the mesoscopic length scale, where the Central Limit Theorem still is not completely effective, so that the coarse grained probability distribution retains some of the features of the microscopic distribution (such as broadness); the macroscopic length scale, where the probability distributions have already renormalized to Gaussians, therefore driving the system to the weak disorder universality class. As a consequence we claim that

the approximation (2.39) will spontaneously hold up to the mesoscopic length scale; imposing it we can extend the strong disorder universality class to any length scale and this will make our arguments neater. We postpone to the next section a more detailed discussion on the dependancy of the universality class of the problem on the probability distribution used, where we will also criticize the above naïve argument.

Coming back to our problem, the ground state configuration of the polymer in strong disorder is then the one corresponding to the path that minimizes expression (2.39), and it is called *optimal path*, with energy E_c (Cieplak et al. (1994)a, Cieplak et al. (1994)b, Roux, Hansen and Guyon (1987)) By definition, when two paths have the same energy E_c, the one which has the lower second maximum is considered to be optimal. If the paths are still degenerate the next maximum has to be analyzed and the procedure must be repeated until the degeneration is completely removed.

The problem of undirected paths with energy (2.39) has been extensively studied by (Cieplak et al. (1994)a, Cieplak et al. (1994)b); as already mentioned, the geometry of the optimal path is fractal with fractal dimension $D_f = 1.2 \pm 0.02$ in $2d$. In (Cieplak et al. (1994)a, Cieplak et al. (1994)b) an algorithm has also been introduced to generate the optimal path. The result of the procedure is an intriguing connection of the polymer in strong disorder with percolation, which will become even stronger for directed polymers.

The algorithm can be described as follows: given a $2d$ lattice, choose a bond at random and eliminate it; sooner or later a bond will be chosen removing which there would be no more connected paths between, say, the left and right sides of the lattice. When this happens another bond must be chosen. This procedure must be repeated until no more bonds can be removed without breaking the connectivity. What has this algorithm to do with the optimal path problem? Simply, assigning a random number (taken from a uniform distribution in $[0, 1]$) to each bond, ranking them in descending order and sequentially eliminating them in that order (taking care not to break connectedness), we are obtaining the optimal path minimizing (2.39).

Of course the resulting path is on the verge of being broken, consequently breaking the connectedness of the remaining bonds. This means that the path lives on a percolating cluster. It would be therefore tempting to associate it with a self-avoiding walk on a percolation cluster. However, it is straightforward to show that the weighting of different connected paths is not the same for the two cases. Indeed, the numerical result $D_f = 1.2 \pm 0.02$ is not consistent with that for a self-avoiding walk on a percolation cluster, for which $D_f = 1.30 \pm 0.01$.

Interestingly enough, an analogous algorithm has been proposed (Newman and Stein (1994)) in the context of spin-glasses. We will come back to this problem in a subsequent section.

Recently, Roux and Zhang (Roux and Zhang (1996)) gave an argument stating that the directed optimal path lives on a directed percolation cluster, and that the ground state energy corresponds to the bond percolation threshold. Moreover, due to degeneracy arguments, they claimed that the characteristic exponents should also correspond to those of directed percolation.

We already mentioned percolation. We now give some more details about it to provide a basic tool we will made use of.

Percolation is a process introduced in 1957 by Broadbent and Hammersley to describe the invasion of water in a porous rock. The easiness with which the fluid can enter a pore is related to the diameter of the channel. A very simple model capturing these essential features is the following. The pores network of the rock is described by a lattice, whose bonds represent the pores. Then the fluid invades a pore with a probability p. Operationally this is implemented assigning to every bond a random number x taken from a uniform probability distribution in the interval $[0, 1]$. Given a bond, it is considered invaded by the fluid if the number $x < p$. The important question to address is whether the invaded bonds form an infinite connected cluster or not. The answer is that there exist a particular value p_c of the probability that a bond is filled with water above which there is such a cluster and below which all clusters are finite. This is a very good and paradigmatic example of geometrical phase transition. As in usual phase transitions the systems displays critical behavior at the transition p_c. In particular we are interested in the correlation length exponent. Defining the correlation function $G(r)$ as the probability that two sites at distance r belong to the same occupied cluster, we write

$$G(r) \sim \frac{1}{r^{d-2+\eta}} e^{-\frac{r}{\xi}} \quad , \tag{2.40}$$

At present we are not interested in the anomalous exponent η. At $p = p_c$ the system exhibits critical behavior because the correlation length diverges (and therefore the exponential approaches a constant, undressing the preceding power law). In particular the correlation length exponent is defined as

$$\xi \sim |p - p_c|^{-\nu} \tag{2.41}$$

In the years many different variations on the same theme of percolation have been proposed. We are particularly interested in two of them: specifically, directed percolation and invasion percolation. The former will be dealt with in this section, and therefore we describe it in the following lines. The second one will be useful in the next chapter, and we postpone its introduction at a more proper time.

Directed percolation can be introduced as ordinary percolation, the main difference being that in this case we inquire about the presence of an infinite cluster spanning the lattice with

bonds oriented in a determined preferred direction. As before we can identify a threshold occupation probability p_c above which we find an infinite cluster. Due to the intrinsic anisotropy of the problem, directed percolation introduces two different correlation lengths, $\xi_{||}$ and $\xi_{\perp}$, respectively parallel and perpendicular to the preferred direction of connectivity. Correspondingly there are two correlation length exponents

$$\begin{aligned} \xi_{||} &\sim |p - p_c|^{-\nu_{||}} \\ \xi_{\perp} &\sim |p - p_c|^{-\nu_{\perp}} \end{aligned} \tag{2.42}$$

In view of our interest in the wandering exponent ζ of the optimal path, it is useful to define a wandering exponent for directed percolation, that is, an exponent relating the transverse and longitudinal properties of the critical infinite percolating cluster. First, since we always deal with finite lattices, the percolation threshold will fluctuate on the average around p_c. These fluctuations are related to the size of the system via the scaling law

$$|p - p_c| \sim L_{||}^{-\frac{1}{\nu_{||}}} \tag{2.43}$$

which is obtained inverting the first of (2.42) and substituing $\xi_{||}$ with $L_{||}$, since the diverging correlation length will at most be equal to the size of the system. Then we substitute (2.43) in the second equation of (2.42), and obtain

$$\xi_{\perp} \sim L_{||}^{\frac{\nu_{\perp}}{\nu_{||}}} \quad . \tag{2.44}$$

The wandering exponent of directed percolation at $p = p_c$ is therefore $\zeta = \frac{\nu_{\perp}}{\nu_{||}}$.

We can now address more thoroughly the argument of Roux and Zhang.

Given the lattice, to each bond we assign a random number x taken from a distribution uniform in the interval $[0, 1]$ and find the optimal path according to (2.39). Next we turn to the percolation fashion and consider as occupied all the bonds with $x \leq p$ with $p \in [0, 1]$. If $p < p_c$ there is no infinite directed percolation threshold. Therefore the optimal path, which is an infinitely connected structure, will pass through bonds not belonging to any finite cluster. As a consequence $E_c > p$. This situation holds as long as $p < p_c$. The inequality

$$E_c \geq p_c \tag{2.45}$$

follows.

We can transform inequality (2.45) into an equality observing that we are looking for the ground state of the path. Therefore, even if the cutoff p is greater than p_c, the optimal path will just consider the cluster of bonds characterized by $x \leq p_c$, and $E_c = p_c$. Living on a fractal structure, the path will share its properties, such as its wandering exponent $\zeta = \frac{\nu_{\perp}}{\nu_{||}}$.

Our aim is to show both analytically and numerically that this is the case.

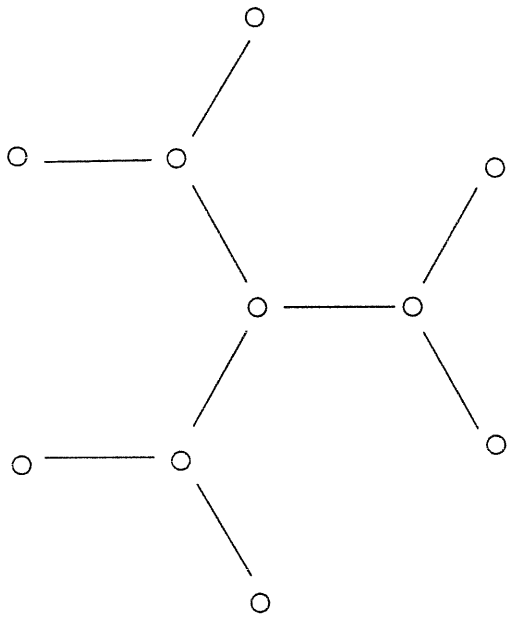

Figure 2.5: Bethe lattice of coordination number $z = 3$

We now show that on the Bethe lattice and on hierarchical lattices the directed percolation thresholds and the energy of the optimal path coincide.

The Bethe lattice (see Fig.2.5) is a branched structure in which each site has z nearest neighbors and in which no two branches are allowed to cross. These very simple properties have profound consequences on the structure of the lattice itself and of the systems arranged on it. In fact the no-crossing rule implies that correlations (and fluctuations) in systems studied on the Bethe lattice will be somewhat neglected. This is a mean-field like consequence. Moreover the fractal dimension of the Bethe lattice is $D_f = \infty$. To check this result we can try to count the number of sites within a range of n lattice steps from a given site. For a d dimensional lattice this number grows like n^d (it is the *volume* of the lattice). On a Bethe lattice the number of sites inside a range of n lattice steps grows exponentially with n. An exponential grows faster than any power, and therefore if we want to write the behavior of this number as n^{D_f} we are forced to use $D_f = \infty$. Actually this is the second feature of the Bethe lattice making it look like a mean-field like structure: it comes as no surprise to discover that the exact solution of many systems on the Bethe lattice is exactly the mean-field solution in the pair (Bethe) approximation.

We didn't emphasize the word *exact* in the lines above, but its presence is very important, because in fact many systems allow an exact solution on Bethe lattices, and the approach is again mean-field like. It is in fact possible to write self-consistent relations for the quantities of interest using the self-similarity of the lattice (that is, the lattice looks the same going down along any of its branches, and branches are independent one from the other).

The first step to prove that the optimal path in strong disorder and directed percolation coincide is to find the proper quantities to be analyzed. For directed percolation this quantity is the probability $P(p)$ of a site to be connected to the infinite percolating cluster.

On the Bethe lattice bonds are oriented from a generation to the next one. Two sites are connected if an oriented path of occupied bonds joins them. Then, calling p the probability that the bond is occupied, the self-consistency equation for $P(p)$ is easily obtained examining the probability that a site is not connected to the infinite cluster, $1 - P(p)$. The probability to be connected through one of the $z - 1$ sub-branches (remember that we oriented the bonds, so that each site has 1 parent site and $z - 1$ descendent sites, which sum up to z neighbor sites) is the product of the probability p that the bond connecting the site to its first descendent is occupied and the probability that the descendent is connected to the infinite cluster, which again is $P(p)$ invoking the self-similarity of the lattice. The probability that the site is not connected to the infinite cluster through any of its sub-branches therefore is $(1 - pP(p))^{z-1}$, and the self consistency relation becomes

$$P(p) = 1 - (1 - pP(p))^{z-1} \tag{2.46}$$

Since at the threshold $p = p_c$ there is a second order phase transition, and $P(p)$ is the order parameter, we can expand (2.46) for small $P(p)$, and it can be found that the percolation threshold is $p_c = 1/(z-1)$[1]. In the case of the optimal path the key quantity is the probability of a path with an energy less than E to propagate *ad infinitum*, never traversing bonds of higher energy. Assigning a uniform random energy between 0 and 1 to each bond. the self-consistency equation we get for the path is the same as for percolation, just changing the probability p that a bond is occupied with the energy E of the path; then of course the energy of the optimal path (the smallest energy for which there is a non zero probability of propagation) is equal to the percolation threshold. The identification of the propagation probability as the key one to study the optimal path is very important, because it can be used also on the diamond hierarchical lattice (Berker and Ostlund (1989)) shown in Fig.2.3. In fact, we can perform an exact renormalization group on this lattice: the probability that a path of energy less than E propagates through a bond must be the same as the probability of propagating through the diamond.

In view of comparing our numerical results for d-dimensional cubic lattices, we perform a general RG transformation where the single bond has to be substituted by a N-sides diamond, where $N = 2^{d-1}$ (see Fig.2.3). We directly work with the energy language of optimal paths. We can write a general expression for the RG equation for the probability $p(E)$ that a bond has an energy less than E. The renormalized probability is then

$$p'(E) = 1 - (1 - p^2(E))^N \tag{2.47}$$

[1] Notice that this threshold is the same as in the case of ordinary (undirected) percolation (Stauffer and Aharony (1992))

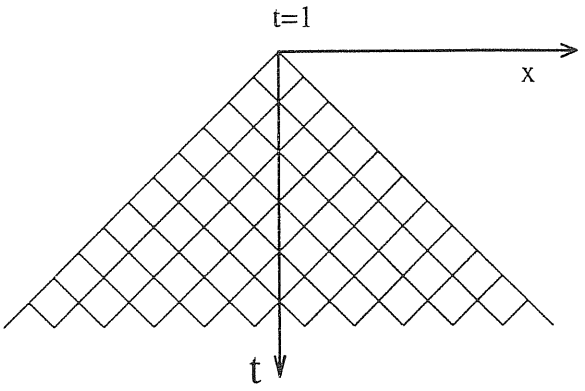

Figure 2.6: Directed square lattice used for numerical simulations.

with initial condition $p(E) = E$.

This is exactly the same recursion as the one for p for directed percolation (which again is the same as ordinary percolation) on these lattices. For $d = 2$ we find

$$E_c(d = 2) = \frac{\sqrt{5} - 1}{2} = 0.6180\ldots \tag{2.48}$$

which is the golden mean. In $d = 3$ the energy of the optimal path is $E_c = 0.2818\ldots$ (notice that in the limit $d \to \infty$ $E_c \sim 1/N$, a behavior different from the Bethe lattice result which is the correct one at order $1/d^2$ with $z = 2d$).

We didn't argue anything about the wandering properties of the optimal path on Bethe and hierarchical lattices because they are ill defined. In fact both the Bethe and hierarchical lattices lack transverse metric properties.

We now discuss the numerical simulations on square and cubic lattices using transfer matrix techniques. We explain the algorithm on a two dimensional lattice, its generalization to any dimension being straightforward. In Fig.2.6 a portion of the lattice is shown, where the diagonal represents the time axis. We are interested in the optimal path connecting a site at $t = t_i$ to an arbitrary site at time $t_f > t_i$. Rows t and $t + 1$ of the lattice (Fig.2.7) are connected by $2t$ bonds, a uniform random value between 0 and 1 is assigned to them. The energies of the optimal paths connecting each site of row $t + 1$ to a site of the top line are obtained via the following algorithm:

$$E_j = min[max(E_i, \epsilon_{ij}), max(E_k, \epsilon_{kj})] \tag{2.49}$$

where E_i, E_k are the energies of the optimal paths connecting the first row to sites i and k respectively; ϵ_{ij} and ϵ_{kj} are the energies of the bonds linking sites i and j, k and j respectively. Assigning a zero energy to the sites of the first row, and then appling the algorithm (2.49), the *true* optimal path energy is the minimum of the energies of the sites of the last row. In order to obtain an homogeneous set of data, we have performed our simulation

by keeping fixed the ratio t_f/t_i between the final and the initial row. For computational convenience we have chosen $t_f/t_i = 1000$ and t_i ranging from $10 < t_i < 300$ in $d = 2$ and $t_f/t_i = 10$ and $10 < t_i < 50$ for $d = 3$. We have analyzed the non-linear sequences $E_c(t_i)$ with standard extrapolation techniques (e.g. Brezinski's θ algorithm(Brezinski (1971)), BST algorithm (Henkel and Schütz (1988)))and we obtained $E_c = 0.6447 \pm 0.0001$ in two dimensions and $E_c = 0.291 \pm 0.002$ in three dimension. These results are in excellent agreement with the best estimates existing in the literature: $p_c = 0.644701 \pm 0.000001$ (Essam, De'Bell, Adler and Bhatti (1986), Essam, Guttmann and De'Bell (1988)) in $d = 2$ and $p_c = 0.28730 \pm 0.00006$ (Grassberger (1989)) in $d = 3$.

These results are strikingly close to the ones obtained on the hierarchical lattices of the same fractal dimensions. This is a further confirmation of the reliability of the calculations on hierarchical lattices and of the insight they provide us.

We also investigate the roughness properties of the optimal path, defined as the end-to end perpendicular displacement of the path. A major difficulty in this case is that the path characterized by the energy (2.39) is highly degenerate, so that it is not possible to doubtlessly identify the end-to-end displacement of the optimal path. The sources of degeneracy are the so called *neckties*, where the incoming path, with energy E, finds more than one way to go to the bottom line without increasing its energy. One way out of this problem could be to compare the second, third energy maxima, and so on, choosing the *true* optimal path as the one with the lowest maxima at any order.

A modification of the previously described transfer matrix algorithm, consisting of a backward scan of the lattice, allows to implement a very efficient way to avoid the problem of the high degeneracy.

In the new algorithm a two dimensional vector is assigned to each site i: the first entry E_i is the energy of the optimal path from that site to the bottom and the second one, X_i is the transverse coordinate of the extremum of the optimal path at the final time.

The procedure starts at the bottom of the lattice where at the generic site i the energy E_i is chosen to be 0 and $X_i = x_i$, the transverse coordinate of the site i itself. Then the updating of the vector assigned to a generic site k at time t is done in terms of the two vectors associated to sites l and j at time $t + 1$, shown in Fig.2.7, according to the rules

$$E_k = min[max(E_j, \epsilon_{jk}), max(E_l, \epsilon_{lk})]. \tag{2.50}$$

$$X_k = \begin{cases} X_j & \text{if} \quad E_k = E_j \\ X_l & \text{if} \quad E_k = E_l \end{cases} \tag{2.51}$$

This procedure gives the optimal path from each site at time t_i to the final time t_f. For simplicity we let the algorithm go with the time-step $\Delta t = 1$. The genuine Roux-Zhang conjecture states that the optimal path lives on the directed percolation cluster on an

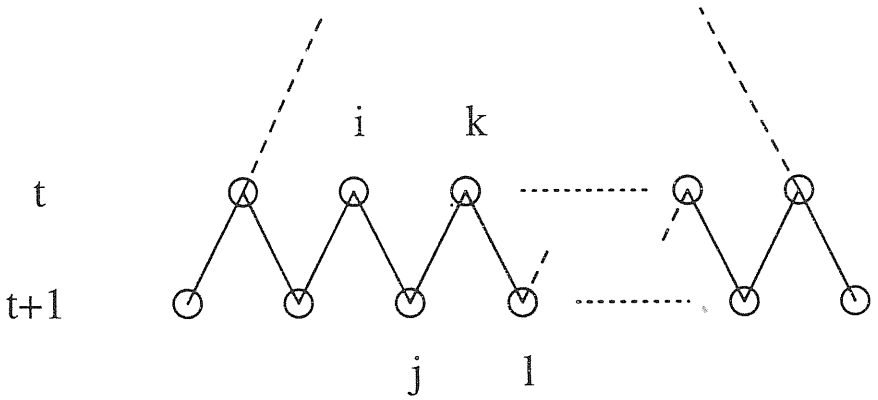

Figure 2.7: Detail of the square lattice.

infinite lattice, which was the asymptotic situation for the threshold calculation setup. The setup for the calculation of the roughness is somewhat different, and the optimal path can be seen as having a fixed extreme. If the fixed extreme lies on the percolation cluster, then the Roux-Zhang argument is valid; else the path travels until it meets the directed percolation cluster: from there on it never abandons it. As a consequence, apart from an initial transient, the roughness of the path is bounded by the width of the percolating cluster. The energy, instead, is in general greater than or equal to its true value, due to an initial regime before contact with the percolation cluster is made, so that it will be different from the percolation threshold.

Using the above described algorithm, we are able to give a very precise estimate for the roughness W of the path defined as the transverse displacement of the optimal path at time t. Given the scaling law for W

$$W \sim t^{\zeta}, \tag{2.52}$$

the exponent ζ is related to the correlation length exponents of directed percolation via the formula (Roux and Zhang (1996))

$$\zeta = \frac{\nu_{\perp}}{\nu_{||}}. \tag{2.53}$$

Indeed in directed percolation, at the critical threshold p_c, the percolating cluster is anisotropic and characterized by two correlation lengths, $\xi_{||} \sim |p - p_c|^{-\nu_{||}}$, in the time direction, and $\xi_{\perp} \sim |p - p_c|^{-\nu_{\perp}}$ in the x direction (Kinzel and Yeomans (1981)). Identifying $\xi_{||}$ with t and $\xi_{\perp}$ with W we get (2.52) and (2.53).

Fig.2.8 shows the log-log plot of W versus t up to $t = 6000$ for the 2-dimensional case. From the best fit we get $\zeta = 0.6325 \pm 0.0007$ to be compared with the best result known (Essam et al. (1988)) $\zeta = 0.6326 \pm 0.0002$.

Fig.2.9 shows the corresponding data for $d = 3$. In this case $\zeta = 0.555 \pm 0.008$ is obtained whereas $\zeta = 0.567 \pm 0.008$ (close even if as not in agreement as in the $d = 2$ case to the

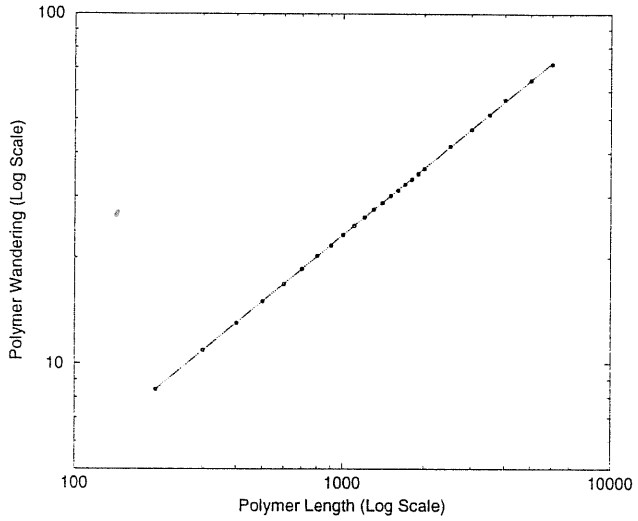

Figure 2.8: Log-log plot of the wandering of the optimal path vs. the final time in $d = 2$.

previous results obtained in (Grassberger (1989)) using Monte-Carlo simulations).

In conclusion we have given quite convincing numerical and analytical evidence that the directed optimal path (Cieplak et al. (1995)) has a roughness exponent related to correlation length indices of directed percolation (Roux and Zhang (1996)). For this purpose a new and efficient transfer matrix algorithm was necessary which allowed excellent estimates of exponents within 0.01% and 0.2% in $d = 2$ and $d = 3$ respectively. Since directed percolation has an upper critical dimension $d_c = 4$ (actually, $4 + 1$) (Cardy and Sugar (1980)) we thus expect this is also the case for the directed extremal optimal path (*i.e.* when $d > d_c$, $\zeta = 1/2$ like standard random walks).

2.4 Changing the energy probability distribution

The results in the previous section raise the question on what is the effect of different probability distributions on the universality class of polymers whose energy is defined as from Eq.2.38. We have given an argument according to which any distribution with finite first and second moments should not change the universality class from weak-disorder. This conclusion prompted us to introduce (2.39) as a definition of the energy in order to preserve the universality class of directed percolation against the Central Limit Theorem on any length scale. Is it possible to find an energy probability distribution such that the universality class is still the directed percolation one using (2.38) even in the thermodynamical limit?

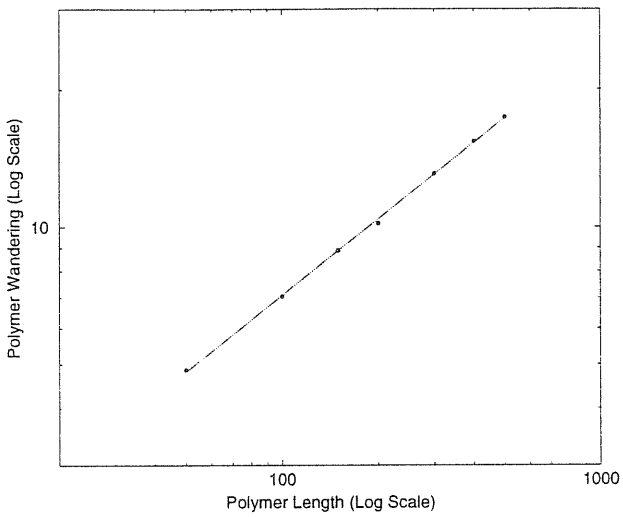

Figure 2.9: Log-log plot of the wandering of the optimal path vs. the final time in $d = 3$.

This question admits a partially positive answer, in fact if the energies are chosen as

$$E = y(c^{L^d})^{y-\frac{1}{2}} \tag{2.54}$$

with y uniformly distributed in $[0, 1]$, and $c \geq 1$ then it is possible to observe a crossover between weak and strong disorder both with c and with L, the size of the system (whose dimension is d): if $c = 1$ the universality class is always the weak-disorder one; if instead $c > 1$ it is possible to identify a crossover length L of the system such that above it the fractal behavior is recovered. Such length gets smaller as c is increased.

A different route to change the universality class of directed polymers has been proposed by (Marconi and Zhang (1990)) starting from the consideration that the problem itself is not Markovian, because it is a global optimization problem, to solve which it is necessary to know the whole hystory of the system. Therefore it is not necessarily subject to the Central Limit Theorem. As a consequence, whereas it is very plausible that any distribution with all the moments that are finite (such as a Gaussian or a uniform distribution in a finite interval) still are in the weak disorder universality class, it is not surprising as well that a distribution with only a finite number of finite moments gives a universality class which is different from the weak disorder one. Such distributions were chosen of the form

$$P(E) \sim \frac{1}{|E|^{\mu+1}} \quad |E| \to \infty \tag{2.55}$$

with $\mu > 2$ to guarantee that the variance of the distribution is finite. This requirement evidently implies that the $1d$ problem does not distinguish between these distributions and

the weak disorder ones. In fact in $1d$ we can give the exact solution for a lattice of length L (measured in lattice steps of length 1). The energy of the polymer is simply given by

$$E = \sum_{n=1}^{L} E_n \tag{2.56}$$

with E_n distributed according to (2.55). The average energy is obviously $< E >= 0$ for symmetry. The variance of the energy is given by

$$\sqrt{< E^2 >} = \sqrt{\sum_{n=1}^{L} < E_n^2 >} = L^{\frac{1}{2}} \sigma_\mu \quad , \tag{2.57}$$

where σ_μ is the variance of (2.55). The $\frac{1}{2}$ exponent in (2.57) is the expected Central Limit Theorem result. Changing μ we do not change the universality class of the system; only the amplitude σ_μ gets changed. The result that if $d > 1$ the universality class changes is profoundly instructive: in fact it means that as soon as the polymer has choices (as in $d > 1$), it fully explores the tails of the energy distribution. Simulations in $d = 2$ yeld values of the wandering exponent larger than $\frac{2}{3}$, which is not surprising because the polymer fluctuates more in search of lower energy bonds that are more common with distributions such as (2.55) than with Gaussians. The energy fluctuations exponent ω is expected to still obey the law $\omega = 2\zeta - 1$ which comes from Galilean invariance (using the mapping of the problem to KPZ equation). It would not hold for time correlated disorder, that is for disorder correlated in the longitudinal direction of the polymer.

Another interesting outcome of this problem is that as $\mu \to 2$, $\zeta \to 1$, that is, the polymer is driven on the verge of fractality, which does not emerge because of the intrinsic transfer matrix setup used in (Marconi and Zhang (1990)) (which imposes the directedness constraint). Yet crossing over from $\mu < 2$ to $\mu \geq 2$ introduces Levy distributions in the problem (see Appendix 1). Since undirected polymers in the strong disorder limit have been shown to follow fractal geometries, using Levy distributions is suggestive of a possible route to cross over from weak to strong disorder.

Another direction we can pursue to introduce new effects, thus changing the universality class of the system is to use distributions with underlying topological properties, such as bimodal distributions.

2.5 Polymers on a bimodal energy landscape

Directed polymers (DP's) in random media (Kardar and Zhang (1987)) have been one of the major topics in the study of disordered systems in the last decade: the universality class of the ground state has been established, as well as its connections in two dimensions with other problems such as domain walls in dirty ferromagnets (Huse and Henley

(1985)), the dynamics of growing interfaces governed by the Kardar-Parisi-Zhang (KPZ) equation (Kardar et al. (1986)) and the Burgers equation of fluid motion (Forster et al. (1977)). In the case of weak disorder all these problems have been recognized to belong to the same universality class, characterized by two exponents that for DP's are the wandering exponent $\zeta = \frac{2}{3}$ and the energy fluctuation exponent $\omega = \frac{1}{3}$ (Huse and Henley (1985)). The two exponents are related in any dimension via the simple relation $\omega = 2\zeta - 1$. Behind the weak disorder universality class there is always the assumption of a distribution of disorder which is narrow around its average, such as a Gaussian. Only more recently some attention has been devoted to the effects of different distributions of disorder on the universality class of DP's.

A very simple and intuitive argument could be set up to show that any distribution with finite first and second moments should belong to the universality class of DP's: since the systems exhibits scaling behavior, some coarse graining steps should not change it: if the first and second moments of the original microscopic distribution are finite the Central Limit Theorem guarantees that the coarse grained disorder distribution converges to a Gaussian, and therefore the system belongs to the weak disorder universality class.

Although convincing, the preceding argument neglects the intrinsic extremality of the problem: in order to minimize the energy, the polymer explores also the tails of the distribution. Therefore it would not be surprising to find that distributions which should obey the Central Limit Theorem (having finite first and second moments) actually fail to be in the weak disorder universality class since they have infinite higher moments. This effect has indeed been observed (Marconi and Zhang (1990)). It is an even less surprising result that when the disorder distribution is so broad that (on the average) the sum of a certain number of variables from that distribution can be well approximated by the largest one, then the so called strong disorder limit is recovered (Cieplak et al. (1994)a), where the universality class has been identified as being the same as directed percolation (Rios, Caldarelli, Maritan and Seno (1996)).

Recently Lebedev and Zhang (Lebedev and Zhang (1995)) concentrated their attention on a bimodal distribution of disorder: to every bond is assigned an energy that can be either 0 or 1 with assigned probabilities,

$$P(E) = p\delta(E) + (1-p)\delta(E-1). \tag{2.58}$$

Even if the bimodal distribution of disorder is characterized by finite moments of any order, it introduces new topological features in the system. If $p \geq p_c$, the directed percolation threshold, then the polymers will lay on the directed percolation cluster, avoiding all the 1-bonds and there will be no energy fluctuations associated with them. If $p = p_c$ the incipient percolating cluster (IPC) is a fractal, and the polymers will share the same wandering properties of the backbone, with $\zeta_p = 0.6326 \pm 0.0002$ (Essam et al. (1988)). Below p_c

there is no infinite cluster spanning the lattice, and the polymers will pick up some 1-bond. Lebedev and Zhang unexpectedly found that the directed percolation universality class extends also for $p < p_c$. They interpreted their data arguing that below p_c the polymers still see the IPC: the 1-bonds that break its connectedness can be seen as disorder on it. It has been shown that polymers forced to live on the IPC with a random energy on the allowed bonds have $\zeta = \zeta_p$ (Balents and Kardar (1992)).

A careful renormalization approach (which can be made exact on hierarchical lattices) shows that if $p < p_c$ the probability to find an infinite connected path of 0-bonds vanishes increasing the length of the lattice (or, which is somehow equivalent, performing some coarse graining step). Therefore on long scales the IPC disappears completely, and polymers will simply be subject to a disordered energy landscape. The previous scaling argument can be applied and the polymer ground state should belong to the weak disorder universality class. since all the moments of (2.58) are finite. This is consistent with (Derrida and Griffiths (1989)), where computations on hierarchical lattices of any (effective) dimension using a bimodal disorder distribution (taking care that the lower energy do not percolate) have been compared to the $(1+\epsilon)$-dimensional expansion with a Gaussian distribution, showing a perfect agreement.

In order to set out this controversy, we performed simulations on euclidean lattices of length up to 2^{13} and taking averages over 10000 realization. The results are shown in Fig. 2.10. Data for $p = 0.3 < p_c$ clearly show the weak disorder universality class with a wandering exponent $\zeta = 0.666 \pm 0.002$, whereas for $p = p_c = 0.6447$ the wandering exponent is very close and compatible with ζ_p.

Therefore, at variance with (Lebedev and Zhang (1995)), we conclude that a bimodal distribution of energies over the bonds does not change the universality class from weak disorder.

2.6 Applications of extremal disorder

We introduce in this section two applications of strong (extremal) disorder that will bridge us smoothly to the next chapter.

2.6.1 A bound for the upper critical dimension of directed polymers in weak disorder

The problem of finding the upper critical dimension of directed polymers in weak disorder attracted some attention mainly because of its connections to problems of surface growth described by the Kardar-Parisi-Zhang equation. Trying to figure out this dimension directly

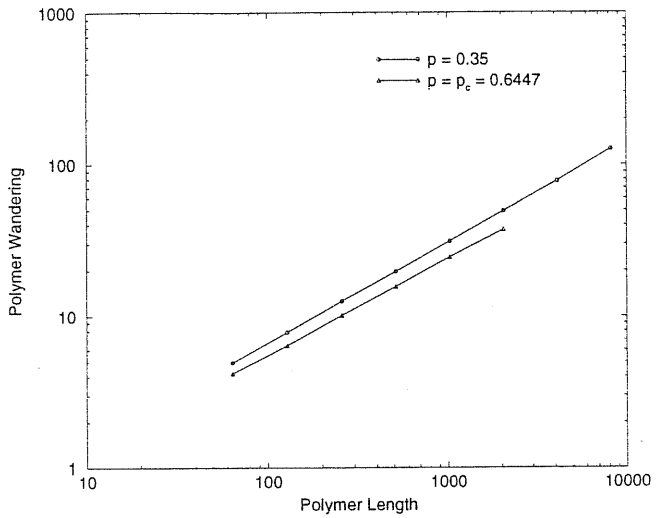

Figure 2.10: Wandering of directed polymers for $p = 0.3 < p_c$ (squares) and $p = p_c$ (circles). Error bars are smaller than the symbols. The wandering exponents are $\zeta = 0.666 \pm 0.002$ ($p = 0.3$) and $\zeta = 0.633 \pm 0.003$ ($p = p_c$).

working on the KPZ equation proves to be a very difficult analytical and numerical task. On the contrary the framework of directed polymers is much more tractable both with theoretical arguments and with numerical efforts.

A directed polymer in a random environment is a highly correlated object, correlations along the polymer coming from its search for the lowest energy bonds in the landscape. We can thus interpret the upper critical dimension as the dimension above which these correlations become irrelevant: the polymer turns to a simple directed random walk whose wandering exponent is well known to be $\zeta = \frac{1}{2}$. Since the relation (2.17) holds independently of the dimensionality, $\omega = 0$. Before going on, we translate these results in the language of the KPZ equation. The dynamical exponent $z = \frac{1}{\zeta} = 2$ and the time transient exponent $\beta = \omega = 0$, from which we obtain $\alpha = \frac{\beta}{z} = 0$, consistently with the relation $\alpha + z = 2$ coming from galilean invariance (and thus independent of the dimensionality of the system). We therefore find out the meaning of the upper critical dimension for the KPZ equation: the system becomes purely diffusive ($z = 2$) as for the Edward-Wilkinson equation, the roughness of the surface does not increase in time ($\beta = 0$) and does not depend on the scale we look at the system ($\alpha = 0$). A flat surface will remain flat at any time and on any scale.

Actually, for some time it has been conjectured if any upper critical dimension exists at all for these problems. At last it has been argued that the upper critical dimension of the KPZ equation is 5 (4 + 1) (Halpin-Healy and Zhang (1995), Moore, Blum, Doherty,

Marsili, Bouchaud and Claudin (1995)). Analytical work in this direction has been done both directly on the KPZ equation and on directed polymers.

Numerical approaches (Ala-Nissila, Hjelt, Kosterlitz and Venäläinen (1993)) are still unconclusive, their prevailing outcome being anyway that there is no upper critical dimension for both KPZ equation and for directed polymers in weak disorder.

We describe here a simple intuitive argument (Cieplak, Maritan and Banavar (1996)). supported by numerical simulations, that, without the ambition of yelding the exact value of the upper critical dimension, gives an upper bound for it.

Let us start from the Eden growth model, which has been well studied in the biological context of the formation of cell colonies such as tissue cultures or bacterial growth. The rule of the model is as follows: given a cluster of bonds on a lattice, choose an interfacial bond at random and occupy it, avoiding loops. This procedure gives rise to a compact structure whose surface shows the same scaling behavior as KPZ equation, characterized by a dynamical exponent z_{KPZ}. In simulations the cluster is grown starting from a central seed. Looking at the wandering exponent ζ of the strand that first reaches a distance L from the seed, the striking result is that $\zeta = \frac{1}{z_{KPZ}}$ as for polymers in weak disorder. The impossibility of the cluster to grow on already occupied sites can be considered as a sort of *annealed* disorder self-generated by the structure during its own growth. Analytical arguments have been presented in the literature whose conclusion is that the strands of Eden clusters are in the universality class of polymers in weak *quenched* disorder (Roux. Hansen and Hinrichsen (1991)). This result has been numerically verified up to $d = 4$.

The lesson we learn from directed polymers in a *quenched* disorder environment is that their wandering is larger than that of their *annealed* version (the simple random walk). This is intuitively explained thinking that the polymer is exploring as much as it can of the landscape in order to find the low energy bonds without increasing too much its length. We trust our insight, and we draw the conclusion that this rule is a good general principle. Therefore we argue that the strands of a quenched version of the Eden model should have a larger wandering exponent than that of the annealed one.

Is it possible to formulate a quenched disorder version of Eden growth? The answer to this question is affirmative, and the name of the game is *Invasion Percolation* (Wilkinson and Willemsen (1983)), a model we already mentioned earlier and whose description we delayed until now.

Imagine we have a porous rock occupied by some fluid A, and we wish to pump inside another immiscible fluid B. The *invader* B will, little by little, push the *defender* A away. The dynamics of the system is mainly restricted to the contact interface between A and B: Invasion Percolation is a simple model that catches the essential ingredients of this dynamics. Intuitively, fluid B advances displacing fluid A searching the easiest way to do so, therefore

invading those channels in the rock where it finds less resistance (due to all the possible microscopic physical effects at play). A very simple way to describe this phenomenon is through a percolative picture. Again we describe the pore network of the rock as a lattice. To every bond of the lattice we assign a random number in the interval $[0, 1]$ describing how much is difficult for fluid B to invade that bond (0 =very easy, 1 =impossible). Starting from a seed cluster, the growth of the invaded region proceeds at each time step occupying the bond at the interface which is characterized by the lowest random number. In this way an invaded cluster is dynamically grown over the lattice.

The first invaded cluster spanning the lattice has the same fractal dimension of the critical cluster of usual percolation. Moreover, the percentage of invaded bonds on the lattice matches the usual percolation threshold. The system *self-organized* into a critical state, with long-range space correlations. This is the first case we meet of a self-organizing system.

As well as the strands of the Eden cluster had interesting properties connecting it to directed polymers, also the strands of Invasion Percolation show connections to polymer problems. In particular it is not difficult to convince ourselves that the first strand connecting a given site of the lattice to the central seed is also the optimal undirected extremal path connecting the two sites. This has also been verified numerically. It is a known result that the undirected optimal path is a fractal structure with fractal dimension D_f and with wandering exponent $\frac{1}{D_f}$ (just as for the random walk the wandering exponent is $\frac{1}{2}$ and the fractal dimension is 2).

Eventually we arrived at the connection we were looking for: the strands of invasion percolation are the *quenched* disorder counterpart of the *annealed* disorder strands of Eden growth, which in turn are the *quenched* disorder counterpart of the random walk. This chain of relations can be translated in the following chain of inequalities

$$\frac{1}{D_f} \geq \zeta_{DP} \geq \frac{1}{2} \quad . \tag{2.59}$$

What does this chain teaches us? $d = 6$ is the upper critical dimension of invasion percolation. Above it its strands have a fractal dimension 2, and therefore $\zeta_{DP}(d \geq 6) = \frac{1}{2}$. This relation gives $d = 6$ as an upper bound for the upper critical dimension of directed polymers in weak disorder. This also sets $6 = 5 + 1$ as an upper bound for the upper critical dimension of the KPZ equation.

2.6.2 The upper critical dimension of an extremal spin-glass model

It is worth mentioning another application (Newman and Stein (1994)) of extremal disorder which, apart from shedding some light on an important problem, introduces also another tool we will find useful in the next chapter.

Spin-glasses represent one of the major paradigms in disordered systems physics. The simplest spin-glass model (the Edwards-Anderson model, EA (Edwards and Anderson (1975))) is the Ising model with interactions that can be both positive and negative, according to some probability distribution, let's say a Gaussian centered around 0. There is no exact solution for this model even in low (two) dimensions. Instead there is an exact solution for the corresponding infinite-range (mean-field) model (the Sherrington-Kirkpatrick model, SK, (Sherrington and Kirkpatrick (1975))), whose main feature is to show many ground states. The origin of this behavior was for long time identified with the presence of disorder in the bond strengths and of frustrated spin configurations, that is, configurations where some spin pairs do not satisfy the sign of the their bond strength. One of the strongholds of spin-glass lore was that this picture had to hold even in low dimensions (as usual the mean-field picture describes systems in $d \to \infty$).

To address this important issue it is possible to build up an extremal model of spin-glass that, despite its doubtful physical realism, clearly shows that disorder and frustration alone are not enough to ensure that a multiplicity of ground states is present.

Given a lattice of side L in d dimensions, assign an arbitrary configuration for the spins at the boundary, and random strengths to the bonds, taking them from a uniform probability distribution in the interval $[-1, 1]$.

Next, take the strongest bond over the lattice (irrespective of the sign) and satisfy it (the two corresponding spins will be parallel if it is positive, antiparallel otherwise). Starting from this seed bond, satisfy the strongest bond which is connected to it, and so on taking care not to create loops. This process leads to the growth of a tree much in the same way we described before for invasion percolation. This growth process stops as soon as there is a growth bond connecting the tree to the boundaries. Since boundaries are fixed, flip all the sites belonging to the tree if necessary. Now, select the next strongest bond remaining on the lattice, and use it as the seed for the growth of a new tree. There are two possibilities: either the new growing tree will connect to the previously grown one, and using spin-flip symmetry it will be possible to accomodate it correspondingly, or it will touch the boundaries and also its growth process will stop. Iterating this procedure we can grow many trees on the lattice. Each tree corresponds to a domain in the ground state of the spin-glass. The question therefore arises if these domains overlap in the thermodynamic limit or not. If they do then we must accomodate their relative orientation in order to minimize the interfacial energy: consequently, this constraint will fix the orientations of the domains modulo a global spin flip symmetry, and there will be just a pair of symmetry related ground states; if instead the domains do not overlap (more precisely, their overlap is evanescent), they will be free to assume both the spin-flip related orientations, and the system will have a multitude of ground states.

Which of the two above scenarios actually verifies? It is a known result that branched

structures in d dimensions have a fractal dimension d_f such that $2d_f > d$ as long as $d < 8$. Therefore the intersection between different trees will have a dimension $2d_f - d > 0$, and the corresponding energy will not be negligible: just a pair of ground states will survive; for $d \geq 8$, $d_f = 4$, and the dimension of the intersection between different trees will be 0, and we will be allowed to neglect the associated energy: in this case the spin-glass will show a multitude of ground states. We conclude therefore that $d = 8$ is the upper critical dimension above which the mean-field (SK) picture of spin-glasses is valid for this model.

This result clearly shows that disorder and frustration alone are not enough to ensure the presence of a multitude of ground state.

Although this second application of extremal disorder is somehow far from the lines of this work, nonetheless we believe it is very instructive. In fact it shows that a clever use of extremal disorder can provide neat answers to conceptual problems which are not easily solved within the usual schemes; moreover, as a byproduct we introduced branched trees as a tool to investigate the upper critical dimension of some systems.

We will make use of it in the next chapter.

3 Extremal Dynamics

3.1 Introduction

In the previous chapter we introduced a new kind of disorder. Working out its details we found out that it is deeply related to Invasion Percolation, a dynamical problem driven by extremal rules (the choice of the strongest bond at each time step). This is the first example of extremal dynamics we encountered in this work.

In recent years there has been a flurry of activity related to the study of such systems, that found applications in as many different physical contexts as surface growth, creep flow, earthquakes dynamics, river networks, economics and biological evolution. Such a widespread consensus on the importance of extremal dynamics is mainly due to its effectiveness in describing the features of real physical systems. In fact most of these models show the striking ability to self-organize in states that, although subject to the rules of stochasticity, exhibit underlying universal features, giving a first explanation of the great and amazing variety of forms coming out from few simple rules in Nature. These rules are not so strict to determine the shape of things to come, yet they impose subtle themes to the apparently free drawing hand of chance. A very beautiful and instructive example are river networks: of course no two rivers are the same, as it is clearly visible, yet it is not difficult to realize with the naked eye that many of the features of one river can also be found in another one. Actually these similarities can be quantified (looking at quantities such as the amount of water through a stream of given length, the roughness of the main stream and so on), discovering that the same relations (with the same universal numbers!) hold for all the rivers in the world. A universal principle is therefore at work, and a glimpse of its essence has been already caught in the literature (Rinaldo, Rodriguez-Iturbe, Rigon, Ijjasz-Vasquez and Bras (1993), Maritan, Colaiori, Flammini, Cieplak and Banavar (1996)).

Even more recently it has been realized that extremal dynamics can lead to a very special kind of self-organization, that is self-organized criticality (SOC). The system drives itself in a state where long-range space an time correlations are present. The word critical is borrowed from equilibrium statistical mechanics, where it indicates a state where the system shows

power law (long-range) decaying correlations. The above mentioned Invasion Percolation is an example of such SOC system, which naturally tunes itself at the critical point of percolation.

Driven by our interests and taste, we will focus in this chapter on a biological application of extremal dynamics, the Bak-Sneppen model of evolution. It is now worth mentioning in which way this model claims to be related to evolution.

Since the publication of Charles Darwin's *On the Origin of Species*, evolution imposed as a model to explain the variety and adaptation of living beings against such beliefs as creationism and theories such as Lamarck's one (according to which morphological traits could be gained from external intervention: cutting tails to mice and then interbreeding them should have given birth to tailless mice). In the years evolutionary biologists turned to experimantal data to check the validity of the theory. These data could be collected in sediments and rocks from ancient times as fossilized rests of past living creatures. Even if evolution got confirmed from these findings, still some unexplained features remained in the data. Principally, paleontologists did not find a uniform distribution of new species and of morphological changes in the sediments. On the contrary the fossil records where showing long periods of so called stasis, where little or no changes where evident in the existing species, separated by short bursts of activity, where a great number of new species stepped on the stage, others were completely wiped out, and in general evolution seemed to be accelerated. This etherogeneous and punctuated distribution of evolutionary events was believed to be a consequence of some kind of bad luck in recording events in rocks more than as something intrinsic in the dynamics of evolution.

With a 180 degrees change of point of view, in 1972 Gould and Eldredge proposed a new interpretation of the fossil records as being full (and not empty) of data, therefore giving dignity to the long stasis periods as truly no-event periods. After 24 years, compelling evidence has accumulated that *punctuated equilibrium* (this is the name used to describe long periods of stasis, equilibrium, separated by small periods, points, of activity) really is a new enriching ingredient of the game of evolution.

Very recently, punctuated equilibrium has also been experimentally verified on bacterial colonies of *Escherichia Coli* (Elena, Cooper and Lenski (1996)), where it has been observed that under conditions favouring larger bacterial sizes, the average size of an individual of the colony experiences long periods of stasis and then abruptly increases.

How do physicists enter the game? Without any claim of describing real evolution, it was soon realized that punctuated equilibrium comes out in a very simple way from extremal SOC systems.

In the next sections we will introduce and review the model, and we will analyze some of its still unexpolored properties. Last, we will propose a more biologically motivated model,

which will turn to be instructive about the features of the original model itself.

3.2 The Bak-Sneppen model of biological evolution

How can a physicist build a model of evolution? To start with, we need to define quantities that are biologically significative from one side and easy to deal with from the other. Biologists do use such quantities, and one of the most common is the *fitness* of species. For the moment being it is sufficient for us to interpret the fitness of a species as its degree of adaptation to the given environment. Even if in a subsequent section we will make distinctions between some different definitions that can be found in the literature, the previous definition gives a good intuition for a few more concetps we are going to introduce.

An ecosystem is an ensemble of different species. Each species interacts with the others; these interactions can be cast in some sort of food-chain, where species with the strongest mutual dependence are closer. In a very loose sense we define therefore a concept of neighborood between species, which turns out to be useful since allows us to describe the ecosystem on a lattice. Every point of this lattice is occupied by a species (not single individuals, since evolution as a whole does not affect individuals), characterized by its fitness. The model consists therefore of a lattice on every site of which there is a real number representing the fitness of the species occupying that site.

We must now describe the rules of the model. To this aim we turn to a concept biologists call *evolutionary pressure*, which characterizes species with a low adaptation (low fitness value) to the environment they are living in: they must evolve or get exctint. In general therefore species with low fitness values will most likely evolve or disappear, and the niche they free will be occupied by some new species. This process results in a change of the fitness of the species occuping that biological niche. According to our definition, fitness is an environment dependent concept. The environment of a species of course includes those species that most interact with it, therefore if one of them changes its level of adaptation (its fitness), the environment of other species will be changed, and their fitness as well.

Since evolution is mainly due to genetic mutations, and the latter occur at random, the simple rule of the system reads as this: choose the species with the lowest fitness, and change it at random according to some probability distribution. Then change the fitnesses of its nearest neighbor as well, according to the same probability distribution.

As it is clear from the rule, this is a model of extremal dynamics. Iterating the process the outcome is absolutely non trivial.

In fact we find that, after a transient, we get the stationary state of the system, where some unexpected features emerge: the probability to find species with fitness values below a threshold f_c is 0, and above it is uniform (Fig. 3.1).

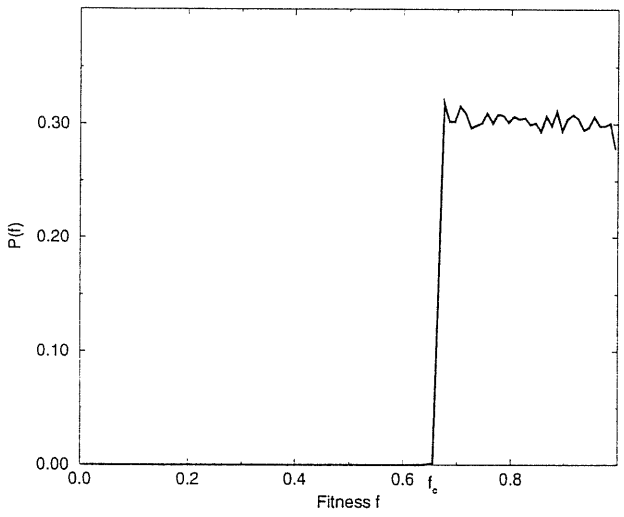

Figure 3.1: Fitness probability distribution for the one dimensional BS model.

The other striking feature of this model is that it shows power law correlation in space and time. Using the language we introduced before, it self-tuned in a critical state: it is a SOC system. The quantities that characterize the criticality of the model can be better understood if we reach a deeper insight on the behavior of the system.

The choice and mutation of the species with the lowest fitness value and of its neighbors triggers a sequence of causally connected mutation events (an *avalanche*) The distribution of the duration of avalanches has a power law behavior, as can be seen in Fig. 3.2, implying that there is no typical timescale in the evolutionary avalanches. This means that there will be long periods during which just minor evolutionary cascades take place (stasis periods), interrupted by huge avalanches: we find therefore that this model shows the *punctuated equilibrium* feature of real evolution.

There is still one more quantity that characterizes the system, characterizing how often activity returns to a given site, or, to be more precise, the probability that activity is at a given site at time t if it was at the same site at time 0. Actually, there are two probability distributions related to this quantity: the first return probability and the all return probability distribution. Both of these show an asymptotic power law behavior (Fig. 3.3).

We do not enter in more details since we will introduce some more formal definition in the next sections.

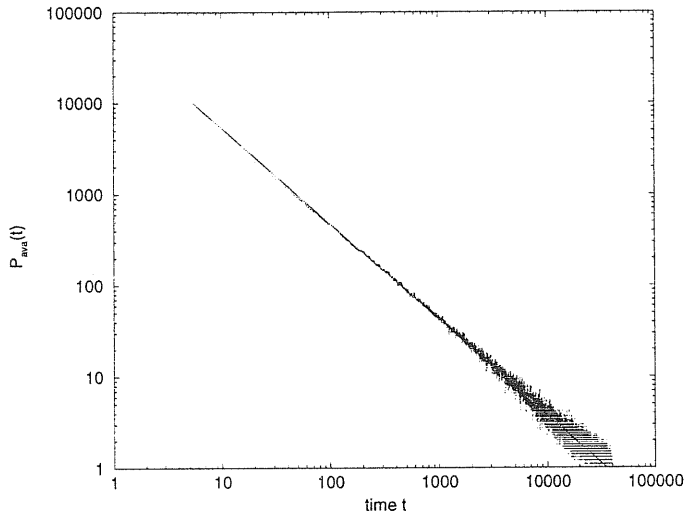

Figure 3.2: Avalanche probability distribution for the one dimensional BS model.

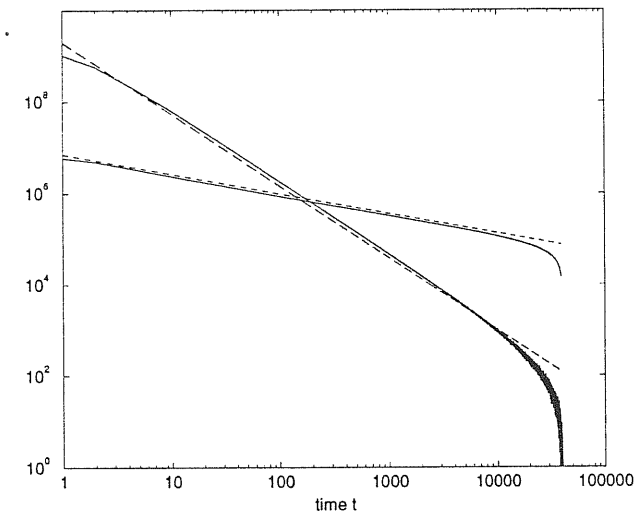

Figure 3.3: Return time probability distributions for the one dimensional BS model: the steepest is the first return time distribution, the other one the all return time distribution

3.3 The upper critical dimension of the Bak-Sneppen model

Much work has been devoted in the last few years to the study of systems that self-organize into a state exhibiting large scale fluctuations and intermittent dynamics. The first simple and instructive model of this type has been introduced in 1987 by Bak, Tang and Wiesenfeld, who proposed a simple mechanism to describe the instabilities and rearrangements of a pile of sand subject to a rain of sand grains (Bak, Tang and Wiesenfeld (1987)). Although the dynamical rules are local and short-ranged, the system self-organizes into a state showing long-range spatial and temporal correlations. Since then it has been argued that similar self-organized critical (SOC) behavior could explain the spontaneous wide occurance in nature of scale-free fluctuation distributions and of the ubiquitous $1/f$ noise. SOC models have been proposed to describe the dynamics of earthquakes (Carlson and Langer (1989)), forest fires (Chen, Bak and Jensen (1990)), fracturing processes (Petri, Paparo, Vespignani, Alippi and Costantini (1994)), river formation and dynamics (Rinaldo et al. (1993), Maritan et al. (1996)) and biological evolution and extinction (Bak and Sneppen (1993)). The common features of all these models is that they show critical behavior without any external fine tuning of the parameters.

Different problems of the physics of SOC models have been addressed in the years. The sensitivity of their universality class to slight changes of the microscopic dynamical rules is still a matter of debate in the case of sand pile models (Pietronero, Vespignani and Zapperi (1994), Ben-Hur and Biham (1996)), whereas it has been shown that biological models change dramatically their behavior as a consequence of new rules (Vendruscolo, Rios and Bonesi (1996)); the effects of disorder and of external temperature-like fields have also been investigated.

The methodological aspects have been also worked out, with the formulation of Renormalization Group (Pietronero et al. (1994), Vespignani, Zapperi and Pietronero (1995)) schemes and of different Mean Field (MF) (Flyvbjerg, Sneppen and Bak (1993), Caldarelli, Tebaldi and Stella (1996)) approaches.

A less studied problem is that of the upper critical dimension of SOC systems.

We will focus in this Letter on the Bak-Sneppen (BS) model of biological evolution. Paleontological data (Raup (1986)) support the picture of evolution as an intermittent phenomenon, which takes place with bursts of activity separated by long periods of stasis (the so called *punctuated equilibrium* (Gould (1977), Eldredge and Gould (1988))). The distribution of the duration of the stasis periods obeys a power law. The idea of punctuated equilibrium has recently been verified experimentally on bacterial colonies of *Escherichia Coli* (Elena et al. (1996)).

In the BS model species are arranged on a lattice in such a way that nearest neighbor

species are those with the strongest mutual interaction in the ecosystem. To each species is assigned a fitness value, which represents the adaptation of the species to the environment. which is taken from a uniform probability distribution in the interval $[0, 1]$. Darwinian selection acts choosing the least fit species as the most likely to evolve or get extinct; its fitness is changed at random according to the same uniform distribution in $[0, 1]$, and so are the fitnesses of the nearest neighbor species. The species self-organize in a state in which there is probability 0 to find species with a fitness value lower than a certain threshold. Moreover evolution takes place in avalanches, that is causally connected mutation sequences. The probability distribution of the sizes s of the avalanches displays a power law decay

$$P(s) \sim s^{-\tau}. \tag{3.1}$$

Activity can be characterized by means of the return time probabilities. If a site is active (it is the least fit one) at $t = 0$, the probability distribution of the waiting times before activity returns in that site for the first time obeys a power law

$$P_f(t) \sim t^{-\tau_f}; \tag{3.2}$$

Also the distribution of the waiting time before a general return (not necessarily the first) has a power law decay

$$P_a(t) \sim t^{-\tau_a} \tag{3.3}$$

and is called the all return probability.

From numerical simulations the values of the exponents are well known in 1 dimension (Figs. 3.1, 3.2,3.3)., $\tau = 1.07$, $\tau_f = 1.57$ and $\tau_a = 0.43$.

There are two significant MF approaches that are worth mentioning. The first one is the Random Nearest Neighbor (RNN) version of the BS model (Flyvbjerg et al. (1993), de Boer, Derrida, Flyvbjerg, Jackson and Wettig (1994), de Boer, Jackson and Wettig (1995)). Within this scheme the nearest neighbor correlations typical of any finite dimension are eliminated choosing the n.n.s of the active site at random over the lattice. This model has been exactly solved and the exponent values are $\tau = \tau_f = \tau_a = 3/2$. A different approach derives from the branching process (BP) picture of the BS model (Caldarelli et al. (1996)). Each active species can be seen as generating new potentially active species. In the approximation that the branching events are not correlated (the MF approximation), one recovers the RNN result.

The difference of the MF results with respect to the $1D$ ones is suggestive of the presence of an upper critical dimension above which the $3/2$ value of the exponents should be found.

In numerical simulations the first and all return probability distributions are much better described than the avalanche probability distribution, because every time step will contribute to the statistics of the formers, whereas the avalanche probability distribution has

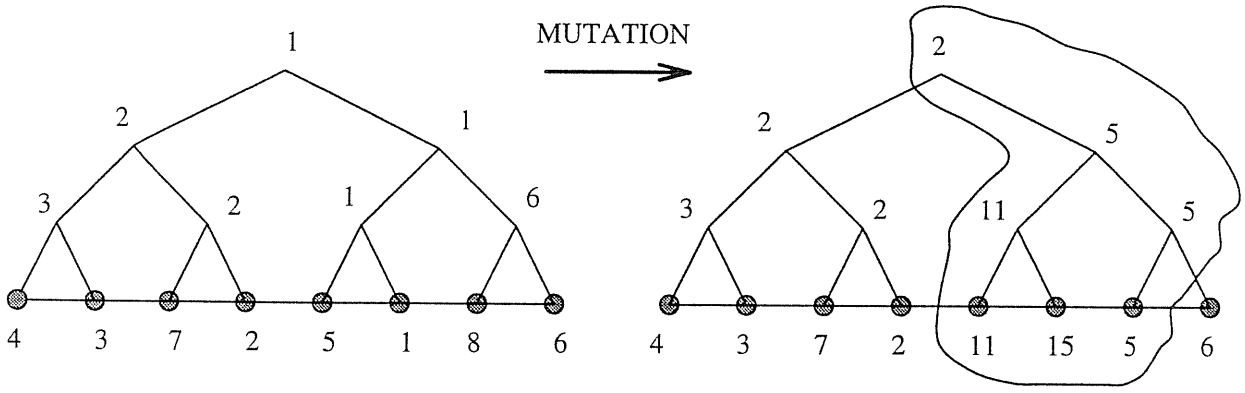

Figure 3.4: Tree algorithm for a one dimensional lattice. After a mutation only a part of the tree must be updated. Since the number of comparisons at any level is at most 3, the time complexity is of order $\log N$. We used integer numbers for sake of clarity.

contributions only at the end of evolutionary avalanches, whose average duration is infinite (as one can easily check from the decay exponent $\tau < 2$). We will therefore concentrate on the determination of τ_f and τ_a.

To this aim we perform numerical simulations in dimensions from 1 to 8. We use a binary tree algorithm as in Grassberger (Grassberger (1995)). We draw a sketch of the algorithm for a one dimensional system in Fig. 3.5. The key idea is to attribute to each site a leaf of the tree; on each node of the tree a number f is stored which is the smaller of the two daughter f's. Thus the smallest f of the whole lattice is stored at the root of the tree, and the corresponding site is obtained by climbing upward until a leaf is reached. After a mutation the tree has to be updated by descending down to the root. Both operations have a time complexity of the order of $\log N$ where N is the number of sites on the lattice.

Resulting data are shown in Table 3.1. The values in $d = 1$ fully recover the known values in the literature.

Several features emerge from our data. For $d \leq 3$ we find $\tau_a \leq 1$, which means that the stochastic process associated with the jumps of the activity over the lattice is recurrent: a recurrent process is a process which has probability 1 to rerturn sooner or later to a site it already visited in the past (this also means that the process will return to that site an infinite number of times or, stated in still another way, that the all return probability is not normalizable in time, as shown by $\tau_a < 1$); $\tau_a > 1$ for $d > 3$, and the process is transient: a transient process is a process which has probability less than 1 to come back to already visited sites (that is, it will come back to those sites a finite number of times). Therefore it is quite natural to define a lower critical dimension d_l separating the two behaviors and such that $\tau_a(d_l) = 1$ (for a simple random walk this dimension would be 2). From our data $3 \leq d_l < 4$: we cannot rule out the possibility that $d_l = 3$ even if $\tau_a(3) < 1$ because at

d_l we can expect logarithmic corrections to the exponents. It could be interesting to build lattices of dimensions intermediate between 3 and 4 (*e.g.* decorated hierarchical lattices) to better locate d_l.

There have been some attempt to find a relation between τ_a and τ_f, yet they don't fit with our numerical data.

We resort to a simple argument for stochastic processes that, in the due approximation, describes our results.

Our starting point is to consider the space-time history of the active site as a random process. In the hypothesis that this process is uncorrelated, some simple arguments provide the exponent laws

$$\tau_f + \tau_a = 2 \tag{3.4}$$

when the process is recurrent and

$$\tau_f = \tau_a \tag{3.5}$$

when the process is transient.

Let $p_n(x)$ be the probability of site x to be active at time n if at time 0 the origin is the active site. Then the following normalization condition holds:

$$\sum_x p_n(x) = 1 \tag{3.6}$$

Define then $f_n(x)$ the probability that the active site is x for the first time at time $n > 0$. The probability that site x is ever active is then

$$F(x) = \sum_{n=1}^{\infty} f_n(x). \tag{3.7}$$

The generating function of $p_n(x)$ is

$$P(x,z) = \sum_{n=1}^{\infty} p_n(x) z^n; \tag{3.8}$$

and the generating function of $f_n(x)$ is

$$F(x,z) = \sum_{n=1}^{\infty} f_n(x) z^n. \tag{3.9}$$

There is a relation between $p_n(x)$ and $f_n(x)$:

$$p_n(x) = f_n(x) + f_{n-1}(x)p_1(0) + ... + f_1(x)p_{n-1}(0). \tag{3.10}$$

Multipling both sides of (3.10) for z^n and summing over n one obtains a relation between the generating functions (3.8) and (3.9):

$$F(x,z) = \frac{P(x,z)}{1 + P(0,z)} \tag{3.11}$$

We are interested in the return probability of the activity at the origin after some time. Therefore we will have $x = 0$ in what follows, and we will omit the coordinate.

Let us suppose that p_n and f_n have a power law behavior with n:

$$p_n \sim n^{-\tau_a} \tag{3.12}$$

$$f_n \sim n^{-\tau_f} \tag{3.13}$$

The probability that activity ever returns to the origin is

$$F(1) = \sum_{n=1}^{\infty} f_n \ , \tag{3.14}$$

Then from (3.11) we can obtain a relation between τ_f and τ_a using Tauberian theorems for generating functions, which relate the behavior of $P(z)$ ($F(z)$) for $z \to 1^-$ to the behavior of p_n (f_n) for $n \to \infty$ and vice-versa. The relations (3.4) and (3.5) follow.

Our data show small deviations from (3.4) and (3.5). Understanding the origin of these discrepacies will be of utmost importance to interpret our data and use them as a guide to find the upper critical dimension of the model.

In fact the argument that led us to (3.4) and (3.5) assumed that the process is uncorrelated. We are dealing with a system that self-organizes in a state where there are long range correlations in space and time. We expect these correlations to induce deviations from the predicted laws. Actually these deviations are indeed observed.

In the light of this conclusion we can therefore interpret the mean-field approximation as the one where correlations, even if present, are irrelevant. The RNN version of the model shows a perfect agreement with (3.5), since $\tau_f = \tau_a = \frac{3}{2}$.

We expect that going to higher dimensions the importance of correlations will get smaller and smaller. If any upper critical dimension is present, above it we should recover the mean-field result. We observe that the correct value appears when $d = 9$. This fixes an upper bound for the upper critical dimension of the BS model.

Indeed we can use the argument further. In fact we observe that (3.5) is violated up to $d = 7$, whereas for $d = 8$ it is compatible with our numbers. We consider this result as a signature of the upper critical dimension more than a sharp $\frac{3}{2}$ value of the exponents. In fact at the upper critical dimension we also expect logarithmic corrections to the exponents, which are difficult to control given the small edge sizes we can deal with, forbidding any finite size consideration. Moreover the $d = 9$ result is so strikingly in agreement with the mean-field predictions that it is very likely to be well above the upper critical dimension.

We conclude therefore that the upper critical dimension of the Bak-Sneppen model is $d = 8$.

d	τ_f	τ_a
1	1.57	0.43
2	1.16 ± 0.01	0.74 ± 0.01
3	1.10 ± 0.01	0.96 ± 0.01
4	1.28 ± 0.01	1.15 ± 0.01
5	1.39 ± 0.02	1.28 ± 0.02
6	1.41 ± 0.02	1.31 ± 0.02
7	1.44 ± 0.02	1.36 ± 0.02
8	1.47 ± 0.02	1.45 ± 0.02
9	1.51 ± 0.02	1.50 ± 0.02
RNN	1.52 ± 0.02	1.52 ± 0.02

Table 3.1: Exponents from the simulations of the Bak-Sneppen model in d dimensions and of the Random Nearest Neighbor Model; These data have been obtained for edge sizes up to 2^{15} ($d = 1$). 2^9 ($d = 2$), 2^6 ($d = 3$), 2^4 ($d = 4$), 2^3 ($d = 5, 6$), 2^2 ($d = 7, 8, 9$). The statistics have been collected from a maximum of $4 \cdot 10^9$ time steps in $d = 1$ to $70 \cdot 10^6$ time steps in $d = 9$.

In order to have some theoretical insight, we resort to the growing trees we already met at the end of the previous chapter. In fact, the dynamics of each avalanche can be seen as the growth of a tree, sprouting new branches from the least fit species. If a branch grows on another branch of the avalanche, changing the random numbers on it also changes the probability of new growth on it, hence it turns out that different branches of the same avalanche actually interact: this is the source of the correlations. Of course, this interactions will be effective as long as the topological conditions of the lattice are such that the intersection between different branches is non negligible. Non-interacting trees are well known to have a fractal dimension $d_f = 4$, therefore their intersections will be irrelevant as long as $d > 2d_f$. Below $d = 2d_f$ intersections between different branches become relevant because their topological dimension is $d_{int} = d - 2d_f$. This simple theoretical argument convinces us that our interpretation of the numerical data is correct, and that $d_u = 8$.

3.4 A model of correlated evolution

Much attention has recently focused upon non equilibrium systems displaying self-organized criticality (SOC), a concept introduced by P. Bak, C. Tang and K. Wiesenfeld (Bak et al. (1987), Bak, Tang and Wiesenfeld (1988)). SOC systems appear to be widespread in nature, including sandpiles (Bak et al. (1987), Bak et al. (1988)), earthquakes (Carlson and Langer (1989)), creep phenomena (Zaitsev (1992)), material fracturing (Petri et al. (1994)). fluid displacement in porous media (Wilkinson and Willemsen (1983), Cieplak and Robbins (1988)), interface growth (Sneppen (1992), Sneppen (1993)) and river networks (Rinaldo

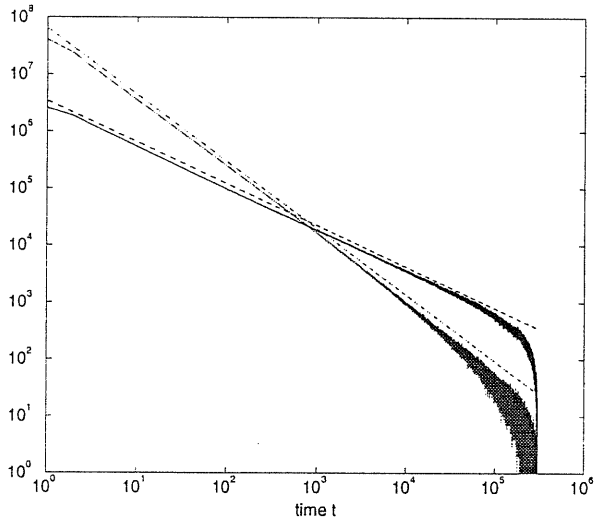

Figure 3.5: Tree algorithm for a one dimensional lattice. After a mutation only a part of the tree must be updated. Since the number of comparisons at any level is at most 3, the time complexity is of order $\log N$. We used integer numbers for sake of clarity

et al. (1993), Maritan et al. (1996)).

Recently Bak and Sneppen (BS) (Bak and Sneppen (1993), Flyvbjerg et al. (1993)) introduced a SOC model describing an ecosystem of interacting species evolving by mutation and selection, and capable of reproducing the punctuated equilibrium features (Gould (1977), Eldredge and Gould (1988)) of evolution as inferred from observations of fossil records (Raup (1986)). The signature of this phenomenon is the power law distribution of evolutionary avalanches, clearly showing that mutations (and extinction) may be episodic at all scales (Gould (1977), Eldredge and Gould (1988), Raup (1986)).

It has been debated if changing the microscopic dynamical rules in the sandpile model does or does not change the SOC universality class of the system (Pietronero et al. (1994), Ben-Hur and Biham (1996)). It is therefore interesting to study the robustness of BS-type models when the interaction rules between species are changed.

In the BS model an ecosystem is represented by N interacting species. Each species is characterized only by its fitness. Such fitness is proportional to the average number of offsprings that an individual of the species may have in the given environment (Peliti (1985)). This definition accounts also for the greater resistance to mutations of the fitter species: mutations must propagate over a greater number of individuals to become a genetic trait of the species.

The species which is the most likely to mutate is the one with the lowest fitness value

because it is the one feeling the strongest evolutionary pressure (it evolves or gets extincted). Genetic mutations, which occur at random, will change the fitness of the species at random as well. A change in the fitness of a species will in turn change the *local* environment for the species that are more dependent on it. As a consequence also those species will change their fitness (which is environment dependent).

It is therefore natural to distinguish between two different mechanisms through which the fitness of a species can change: a primary one due to spontaneous mutations, that involves the species with the lowest fitness, and a secondary (or induced) one, due to changes in the environment caused by the spontaneous mutation of another species. Without the offspring related definition of fitness it would be difficult to really understand why and how primary mutations induce secondary ones (Chau, Mak and Kwok (1995)). In our model such observations translate into microscopic dynamical rules according to which secondary mutations are nontrivially correlated to primary ones.

3.5 The Model

In the BS model species are arranged on a lattice, and interactions are among nearest neighbors. To each species it is assigned a fitness represented by a random number x with uniform probability distribution in $[0,1]$. Evolution takes place in the following way: at each time step the species with the minimum fitness x_i is the most likely to mutate. Thus it is selected and the value of its fitness is redrawn. Together with it, also the fitnesses of its nearest neighbors change at random with the same uniform distribution in $[0,1]$. The BS model does not introduce any correlation between primary and secondary mutations except causality: primary mutations induce secondary ones.

The SOC behavior of the system can be seen from the distribution $P(s)$ of the number s of causally connected mutation events, or avalanches. In $1D$ it is found that $P(s) \sim s^{-\tau}$ (Bak and Sneppen (1993)) and the most accurate numerical estimate of the exponent is $\tau \simeq 1.073(3)$ (Grassberger (1995)). The distribution $P(t)$ of the time t of first return (the interval between two successive mutations of the same species i) displays a power law behavior as well, $P(t) \sim t^{-\tau_{first}}$, with $\tau_{first} \simeq 1.58$. The same observation applies to the distribution of any return, with an exponent $\tau_{all} \simeq 0.42$. An interesting feature of the distribution $P(x)$ of the fitness in the BS model is that species with a fitness below a threshold value $x_c \simeq 0.667$ are likely to undergo a rapid extinction, that is, $P(x) = 0$ for $x < x_c$ (Bak and Sneppen (1993)). Above x_c, $P(x)$ is independent of x.

The BS model can be considered as a food chain where the mutation of a species randomly affects the fitness of its neighbors. It is legitimate to inquire about the motivations and effects of a different microscopic dynamical rule. We introduce a more biologically motivated

correlation between species assuming a predator-prey relation as given *e.g.* by the well known Lotka-Volterra equations (Gardiner (1985)).

If a species increases its fitness, this will affect in different ways the *local* environment of those species that most interact with it. Species that feed on it will find a greater number of preys, and this means that they will have better chances to propagate their genes, and their fitness will be higher than before. On the contrary, preys (or in general competitors), will find a fitter predator or competitor, thus finding a more hostile environment: their fitness will be lower than before. The opposite rule applies in the case the species with the lowest fitness value further weakens. Rules of this kind are often found in the biological literature (Higashi and Nakajima (1995)).

Operationally this implies that if $x_i(t+1) < x_i(t)$ then $x_{i+1}(t+1)$ is extracted in $[0. x_{i+1}(t)]$ and $x_{i-1}(t+1)$ is extracted in $[x_{i-1}(t), 1]$. The fitness of species $i+1$ which is *predator* over species i is decreased randomly and the fitness of species $i-1$ which is the *prey* of species i is increased randomly. In the opposite case when $x_i(t+1) > x_i(t)$ then $x_{i+1}(t+1)$ is extracted in $[x_{i+1}(t), 1]$ and $x_{i-1}(t+1)$ is extracted in $[0, x_{i-1}(t)]$.

3.6 Numerical Simulations

We perform simulations for a $1D$ system with the rules described in Sec.3.5. The correlated model introduced in this paper still shows the presence of a threshold in the distribution $P(x)$. A major difference with respect to the original BS model is that above such threshold $P(x)$ is not a constant. From mean field calculations, that we will discuss in the next section, we expect an algebraic behavior for $P(x)$ for $x \to 1$,

$$P(x) = A(1-x)^{-\alpha}, \tag{3.15}$$

where from the normalization condition, $A = (1-\alpha)/2(1-x_c)^{1-\alpha}$. The fitness probability distribution obtained numerically, shown in Fig. 3.6, is well represented by a power law in the entire interval $[x_c, 1]$. We estimate $\alpha = 0.51(1)$ and $x_c = 0.75(1)$,(note that $P(x_c) \sim 2$). This distribution has a very simple meaning and implies that the greater is the probability to find a species the higher is its fitness.

From scaling analysis of our numerical data, we obtain the avalanche exponent $\tau = 1.04(2)$ (see inset in Fig.3.7).

For the distribution $P_{first}(t)$ of the first return time and for the distribution $P_{all}(t)$ of any return time we obtain respectively $\tau_{first} = 1.40(2)$ as shown in Fig.3.7. and $\tau_{all} = 0.60(1)$. We note that the relation $\tau_{first} + \tau_{all} = 2$ holds within the error as for the BS model (Maslov, Paczuski and Bak (1994)).

The correlated model introduced in this paper belongs to a different universality class from

the BS model. We enquire about its robustness by introducing a second model (Model B, whereas the previous model will be referred to as Model A in what follows), with a modified microscopic rule. The primary mutation induces secondary mutations of the nearest and next to the nearest species in such a way that if it increases its fitness then the two *predators*, that is the two species on the right side, will increase their fitness too; the two species on the left will instead have an alternate behavior, the nearest one decreasing its fitness, the next nearest one increasing it. In the opposite case, when species i decreases its fitness, also species $i+1$ and $i+2$ decrease their fitness as well, whereas species $i-1$ increases its fitness and species $i-2$ decreases it. As odd as it may seem, this rule is just the simplest extension of the before mentioned predator-prey relation.

Simulations of the evolution of this second model show that again the fitness distribution exhibits a threshold and that above it $P(x)$ increases as $(1-x)^{-\alpha}$ with $\alpha = 0.748(3)$ (Fig. 3.6). Again the behavior of $P(x)$ above the threshold seems to be a power law, obeying the law (3.15). The critical exponents τ, τ_{first} and τ_{all} are unchanged within the error. We can thus conclude that the two models belong to the same universality class (which is determined from the avalanche and return time exponents and not from $P(x)$ which is much more like an order parameter).

In order to check the previous results we perform numerical simulations of the random neighbor version of both models, that is, the species that undergo secondary mutations are chosen at random on the left and on the right sides of the one affected by a primary mutation. The results are qualitatively in agreement with those from the nearest neighbor models: the fitness distribution shows both a threshold and a divergence for $x \to 1$, and the divergence exponents agree within the error with those from simulations for the nearest neighbor model. The avalanche and return time exponents are all 1.50(1) for both models, in agreement with the random neighbor version of the BS model and with the theoretical predictions for it, $\tau = \tau_{first} = \tau_{all} = \frac{3}{2}$ (Flyvbjerg et al. (1993), de Boer et al. (1994)). Actually this doesn't come as a surprise, since the random neighbor version of the models can be formulated in terms of branching processes, where the exponents $\frac{3}{2}$ come out independently of the details of the microscopic rules (Caldarelli et al. (1996)).

We thus identify a *mean field* universality class to which the random neighbor versions of the BS and correlated models all belong. The *mean field* predictions for $P(x)$ are quite in agreement with the real behavior of the system, as it should be if we interpret the fitness distribution as some sort of order parameter.

Actually, if this is the case, we expect the mean field approximation to better describe the system far from the critical point, that in this case is the fitness threshold.

3.7 Mean Field Solution

We give a mean field analysis of the models in order to check the divergence of $P(x)$ for x close to 1. We write a master equation for the problem.

$$P(\mathbf{x};t+1) = \sum_{i=1}^{N} \int_0^1 d\mathbf{x}' P_a(i;\mathbf{x}') T(i;\mathbf{x}',\mathbf{x}) P(\mathbf{x}';t) \ , \tag{3.16}$$

where $P(\mathbf{x};t)$ is the probability of the fitness configuration $\mathbf{x} = \{x_1,...,x_N\}$ at time t; $P_a(i;\mathbf{x})$ is the probability that the site i is active given the configuration $\mathbf{x}$,

$$P_a(i;\mathbf{x}) = \prod_{j\neq i} \theta(x_j - x_i) \ ; \tag{3.17}$$

$T(i;\mathbf{x}',\mathbf{x})$ is the transition probability from configuration $\mathbf{x}'$ to configuration $\mathbf{x}$ if i is the active site.

Bak and Sneppen model: only three sites change their fitness, taking it at random from a uniform probability distribution between 0 and 1. Then the expression for $T(i;\mathbf{x}',\mathbf{x})$ is

$$T(i;\mathbf{x}',\mathbf{x}) = \prod_{j\neq i,i\pm1} \delta(x'_j - x_j) \ . \tag{3.18}$$

The mean field approximation turns out to be just an *ansatz* for the form of $P(\mathbf{x})$ at the stationariety (no more time dependence):

$$P(\mathbf{x}) = \prod_{i=1}^{N} p(x_i) \ . \tag{3.19}$$

Substituting (3.19) in (3.16), integrating over $N-1$ of the N possible x_i variables between 0 and 1, and integrating over the last variable between x and 1 we obtain an equation which is the same as the one presented in (Flyvbjerg et al. (1993)):

$$(1 - \frac{2}{N-1})Q^N(x) + \frac{2N}{N-1}Q(x) + 3\,(x-1) = 0 \ , \tag{3.20}$$

where $Q(x) = \int_x^1 p(x')dx'$. The solution of this equation is (Flyvbjerg et al. (1993)):

$$P(x) = \begin{cases} 0 & x < \frac{1}{3} \\ \frac{3}{2} & x > \frac{1}{3} \end{cases} \tag{3.21}$$

In the limit $x \rightarrow 1$ we try a solution of the form

$$p(x) \sim A(1-x)^{-\alpha} \ ; \tag{3.22}$$

Cancellation of the leading terms in the *l.h.s* of (3.20) yields $\alpha = 0$ and $A = \frac{3}{2}$, consistently with (3.21).

Starting from equation (3.16), we can derive a mean field solution for our models changing the transition probability $T(i;\mathrm{x}',\mathrm{x})$.

Model A: three sites are involved in the change, the active one and its two nearest neighbors, as in the BS model. If i is the active site, then the site $i+1$ changes in the same direction, and the site $i-1$ in the opposite one. The corresponding transition probability can be written as

$$\begin{aligned} T(i;\mathrm{x}',\mathrm{x}) &= \left[\prod_{j\neq i,i\pm1}\delta(x'_j - x_j)\right]\cdot \\ &\cdot \left[\theta(x_i - x'_i)\frac{1}{1-x'_{i+1}}\theta(x_{i+1}-x'_{i+1})\frac{1}{x'_{i-1}}\theta(x'_{i-1}-x_{i-1})\right. \\ &+ \left.\theta(x'_i - x_i)\frac{1}{x'_{i+1}}\theta(x'_{i+1}-x_{i+1})\frac{1}{1-x'_{i-1}}\theta(x_{i-1}-x'_{i-1})\right] . \end{aligned} \tag{3.23}$$

The mean field *ansatz* is again (3.19); proceeding through the same steps as before we obtain the following mean field equation:

$$\begin{aligned} &\left(1-\frac{2}{N-1}\right)Q^N(x) + \frac{2N}{N-1}Q(x) + (x-1) + \\ &-\frac{N}{N-1}\int_0^1 p(x')\left[\frac{2x'-x}{x'}\theta(x'-x)+\frac{1-x}{1-x'}\theta(x-x')\right]\left[1-Q^{N-1}(x')\right]dx' = 0 \end{aligned} \tag{3.24}$$

We try a solution of the form (3.22). After some simple algebra, cancellation of the leading terms in the *l.h.s.* of (3.24) gives $\alpha = \frac{1}{2}$, in agreement with both true and mean field simulations.

Model B: this model involves the simultaneous change of five sites, the i site and its nearest and next to the nearest neighbors according to the above mentioned rules.

The transition probability reads

$$\begin{aligned} T(i;\mathrm{x}',\mathrm{x}) &= \left[\prod_{j\neq i,i\pm1,i\pm2}\delta(x'_j - x_j)\right]\cdot \\ &\cdot \left[\theta(x_i - x'_i)\frac{1}{1-x'_{i+2}}\theta(x_{i+2}-x'_{i+2})\frac{1}{1-x'_{i+1}}\theta(x_{i+1}-x'_{i+1})\cdot\right. \\ &\cdot \left.\frac{1}{x'_{i-1}}\theta(x'_{i-1}-x_{i-1})\frac{1}{1-x'_{i-2}}\theta(x_{i-2}-x'_{i-2})\right. + \\ &+ \left.\theta(x'_i - x_i)\frac{1}{x'_{i+2}}\theta(x'_{i+2}-x_{i+2})\frac{1}{x'_{i+1}}\theta(x'_{i+1}-x_{i+1})\cdot\right. \\ &\cdot \left.\frac{1}{1-x'_{i-1}}\theta(x_{i-1}-x'_{i-1})\frac{1}{x'_{i-2}}\theta(x'_{i-2}-x_{i-2})\right] . \end{aligned} \tag{3.25}$$

The mean field approximation leads now to the equation

$$\left(1-\frac{4}{N-1}\right)Q^N(x) + \frac{4N}{N-1}Q(x) + (x-1) +$$

$$-\frac{N}{N-1}\int_0^1 p(x')\left[\frac{4x'-x}{x'}\theta(x'-x)+3\frac{1-x}{1-x'}\theta(x-x')\right]\left[1-Q^{N-1}(x')\right]dx'+$$
$$+\frac{2N}{N-1}\int_0^1 p(x')\left[\int_0^{x'} Q^{N-1}(x'')dx''-x'Q^{N-1}(x')\right]\left[\frac{x}{x'}\theta(x'-x)+\frac{1-x}{1-x'}\theta(x-x')\right]=0. \tag{3.26}$$

In the limit $x \to 1$, using (3.22), we obtain $\alpha = \frac{3}{4}$ again in agreement with both kind of simulations.

We could further generalize the model, allowing N sites to be involved in the mutation event, with a simple extension of the rule that led from model A to model B. In that case we obtain $\alpha = \frac{N-2}{N-1}$. The theoretical limit, as is clearly visible, is $\alpha \to 1^-$ when $N \to \infty$, which ensures integrability of the fitness probability distribution. Since the value of α depends on the number of species involved in the change, we argue that it is also strongly dependent on the dimensions of the system.

The mean field approach we used shows very powerful in the determination of $P(x)$, at least far from the threshold x_c, as we could expect from a mean field solution far from the critical point.

3.8 Conclusions

The recent introduction (Bak and Sneppen (1993)) of a very simple model able to reproduce some of the features that seem to be important to understand the evolution of life, such as *punctuated equilibrium* (Gould (1977), Eldredge and Gould (1988), Raup (1986)), stimulated research both to better understand the properties of the model itself (de Boer et al. (1994)) and to introduce more realistic features (Newman and Roberts (1995)).

We adopted a definition of fitness that allows us to introduce a *predator-prey* correlation among the species, which we believe is an essential ingredient in the description of an ecosystem.

We have presented numerical simulations of two related models based on this dynamics and we were able to describe their behavior using a mean field approach.

The analysis of these new models clearly shows that they are still SOC systems and that they belong to a different universality class than the Bak-Sneppen model. This is an important result, in fact, the BS model turns out to be sensitive to changes of the microscopic dynamical rules. As it has been recently observed this is not a feature characteristic only of SOC models based on extremal dynamics but also of sandpile models (Ben-Hur and Biham (1996)).

Also the fitness probability distribution $P(x)$ is non trivially affected by the introduction

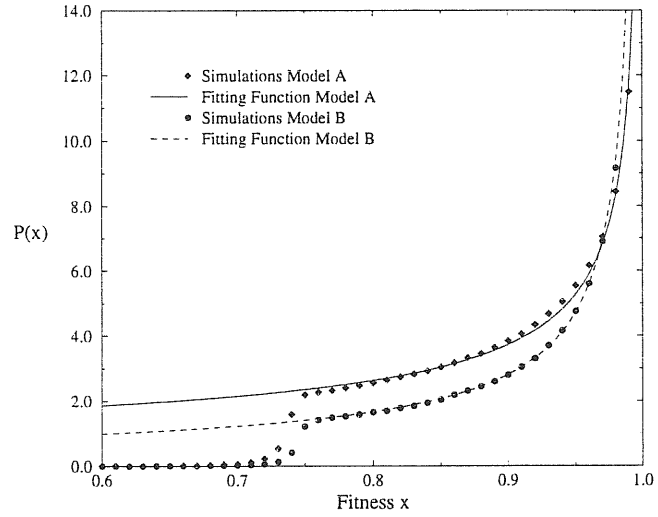

Figure 3.6: Fitness probability distributions for Model A (diamonds) and Model B (circles); symbols correspond to results from simulations ($1D$ nearest neighbor model), the fitting functions are proportional to $(1-x)^{-0.5}$ (Model A, solid line) and to $(1-x)^{-0.75}$ (Model B, dashed line).

of correlations among the species. There are no species with a fitness below a certain threshold (just as in the BS model), and above it there is a higher probability to find species with high fitness values.

The new model can still be considered a branching process, as it is signaled by its mean field exponents. Moreover the law $\tau_{first} + \tau_{all} = 2$ is still respected.

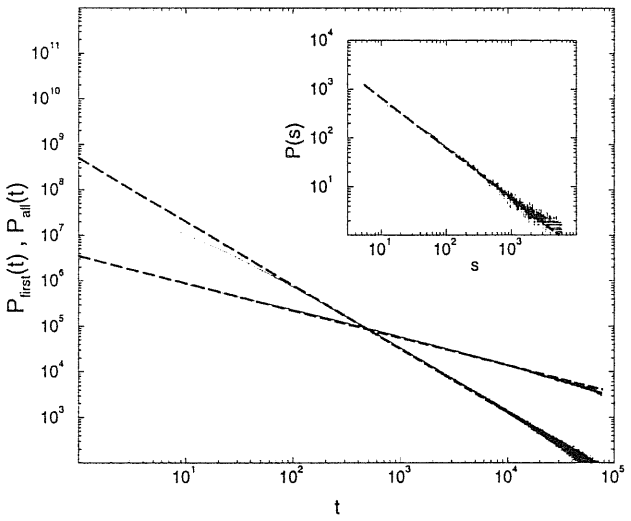

Figure 3.7: Return time probability distributions for model A. We obtain numerically $\tau_{first} = 1.40(2)$ (lower curve) and $\tau_{all} = 0.60(1)$ (upper curve). The avalanche probability distribution $P(s)$ is shown in the inset ($\tau = 1.04 \pm 0.02$)

4 Phase transitions in porous media

The effects of disorder on phase transitions have been a subject of research for a long time. In particular much attention has been paid to the effects of quenched random disorder on the exponents of phase transitions of second order, and on the order of the phase transition itself. To solve these problems a plethora of approaches has been developed, but the one which proved most succesfull is the *droplet* picture of disordered systems. Among the many successes of these schemes it is worth mentioning the Imry-Ma (Imry and Ma (1975)) argument for the ground state of the Random Field Ising Model (Fishman and Aharony (1976)).

The Random Field Ising Model (RFIM) consists of a ferromagnetic Ising model with a random field applied to each site, with Hamiltonian

$$H = -J \sum_{<i,j>} s_i s_j + \sum_i h_i s_i \quad ; \tag{4.1}$$

$J > 0$ and the fields h_i are taken from a distribution of disorder symmetrical around 0. The first question we ask ourselves is if the ground state of this model is ordered. In fact, even if the net field is zero thanks to the symmetry of the distribution of the local fields, nonetheless we can find regions of the lattice with an average field different from zero. In those regions the spins will try to align to the fields, and parallel to each other, thus satisfying also the coupling J. Of course, for every region with a net positive field there will be one with a negative one. Therefore we could naïvely think that the ground state of the system will be just a collection of differently oriented domains, with average global zero magnetization. The ingredient we miss to have a complete picture of the problem is that these domains need interfaces to coexist. Each interface has an energy cost since the spins on opposite sides have opposite spins. Is this energy cost high enough to forbid the formation of domains? To answer this question we must carefully balance the energy gain we get aligning spins inside a domain and the energy loss due to interfaces.

The Imry-Ma argument is just such a balance of energies. The net field inside a domain has a magnitude which is proportional to the fluctuations of the field. Inside a droplet of

N spins the field will therefore scale as $N^{\frac{1}{2}}$. Since $N \sim L^d$, with L the size of the domain and d the dimensions of the system, we obtain that the energy gain due to ordered domains grows as $L^{\frac{d}{2}}$. The energy loss due to interfaces grows instead as L^{d-1} (it has been always conjectured that domains are compact, non fractal, objects). Domain formation will be favourable when $\frac{d}{2} > d-1$, that is $d < 2$, discouraged if $d > 2$. Since the presence of many domains implies that a ferromagnetic order is not stable, *i.e.* the ground state is not ordered. it follows that the one dimensional system does not order (actually of course this do not come as a surprise) and the three dimensional one does. It was later on demonstrated that the system does not order even in two dimensions (Bricmont and Kupiainen (1987)) (the proof was a difficult one but based on a formalization of the Imry-Ma argument). This result was in disagreement with the dimensional reduction argument coming from field theories (Parisi and Sourlas (1979), Parisi and Sourlas (1982)) and stating that the behavior of the $d-$dimensional RFIM is the same as that of the $d-2$ dimensional pure model: according to it the three dimensional model should have not been able to order. The years saw the success of the droplet approach.

A nice and straightforward extension of the Imry-Ma argument led Berker to predict the effect of disorder on first order phase transitions (Berker (1993)). Given a system with first order symmetry breaking phase transitions, let us stay at its critical temperature T_c. There the system exhibits coexistence between a symmetric disordered phase, which is the only stable one at high temperatures, and one or more symmetry-broken phases, stable at low temperature. Disorder induces fluctuations in the local transition temperatures of different domains (the presence of disorder can be seen either as changing the local transition temperature of a domain or as changing the local 'effective' temperature in the opposite direction (Berker (1993))): of course a finite domain does not exhibit any sharp transition. but just a rounded one, and consequently a transition temperature can be identified by smoothed jumps or bumps in the specific heat. If inside a symmetric domain there are regions with a transition temperature $T_c' > T_c$, these regions happen to be at a temperature T_c lower that their critical one T_c', and therefore they will order, with the formation of domains of broken symmetry. The same argument holds within symmetry broken domains. where there could be regions with an smaller transition temperature and a tendency to loose the order. If this situation realizes, then the domain within domain picture of the phase transitions implies that we are loosing a clear cut distinction between the ordered (symmetry-broken) and the disordered (symmetric) phases. We will not be able any more to see coexistence at the phase transition and the transition will turn to second order (it does not disappear because there is not any coexistence to work on at low and high temperatures). It is possible to formulate the above argument in a more precise way just in parallel with the Imry-Ma argument. In fact if the local critical temperature of a domain inside a disordered phase at the coexistence is higher than the pure system critical temperature, then it will order gaining a free energy that scales as $L^{\frac{d}{2}}$ but loosing an interface free energy scaling

as L^{d-1}. Again we find that $d = 2$ is a critical dimension above which first order phase transitions are stable against disorder and at which they are converted to second order. As far as temperature driven first order transitions (they involve phase coexistence between different phases with the same symmetry) are concerned, disorder eliminates the possibility of coexistence and the transition disappears when $d \leq 2$ (there is no symmetry to break between the two phases, henceforth there can not be any second order transition).

The above exposition of the Imry-Ma and Berker arguments has been simplified not to overdress it with too many details. These particular issues can be addressed now that the argument has been clearly stated.

We first notice that above $d = 2$ first order phase transitions are not infintely stable. Whereas for $d \leq 2$ any infinitesimal amount of disorder is enough to transform or eliminate the transition, when $d > 2$ there is a threshold amount of disorder below which the transition is stable and above which it is converted or eliminated.

Second, we observe that if the symmetry of the system is $O(n)$ with $n > 1$ then the interface free energy scales as L^{d-2} and therefore the critical dimension of the arguments becomes $d = 4$. All other considerations can be extended to the $O(n)$, $n > 1$, case.

In what follows we will concentrate our attention on a model describing phase transitions in ^{3}He-^{4}He mixtures. These systems show a particularly rich phase diagrams, with both second order phase transitions and first order ones. Since adding disorder on them is relatively simple, they became one of the most popular arenas for the study of phase transitions in disordered systems.

We will introduce the model and the way disorder can be superimposed on it. Then we will move on to study the system on a Bethe lattice.

4.1 ^{3}He-^{4}He mixtures in aerogel

^{3}He-^{4}He mixtures show a great variety of phase transitions (for a review see (Chan et al. (1996))). First, there is the usual superfluid transition of ^{4}He, which is of second order. The broken symmetry is the symmetry of the wave-function of ^{4}He atoms. In the superfluid phase the phase of the wave-function is uniquely determined over all the system.

Of course the introduction of small quantities of ^{3}He in the pure ^{4}He can itself be seen as a sort of disorder. But, since it has its own energetic properties this 'disorder' variable is correctly counted among the thermodynamic quantities of the system.

How does ^{3}He affect the transition? Given a certain concentration of ^{3}He atoms below a threshold, lowering the temperature the system first undergoes the normal-superfluid second order phase transition, then, at lower temperatures, it splits in two coexisting phases: a

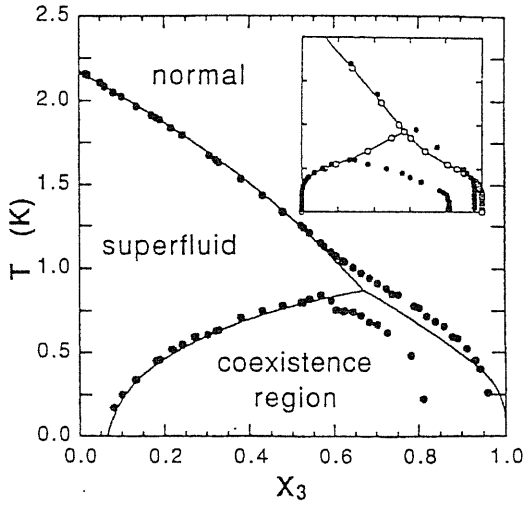

Figure 4.1: The phase boundaries of ^{3}He-^{4}He mixtures in 98% aerogel are defined by closed circles. In contrast to bulk mixtures (solid line), there is no tricirtical point. The figure is from (Chan et al. (1996))

superfluid ^{3}He poor phase and a normal ^{3}He rich phase. This transition is a symmetry breaking first order transition. If the concentration of ^{3}He atoms is above the threshold, the system undergoes only one first order transition, characterized simultaneously by the onset of superfluidity and by the separation of ^{3}He poor and rich phases. (see the continous line in Fig.4.1).

Given the extreme variety of scenarios present in the phase diagrams of these systems, we expect that the introduction of disorder is able to produce new effects.

We can impose quenched disorder on a fluid putting it in a low density porous material. Aerogel is just such an environment. Without going in the details of the production processes of aerogels, we just recall that they are random silica structures with a degree of porosity that can be as high as 99.8% (which means that only the 0.02% of the space occupied by the aerogel is occupied by silica; all the rest is empty space, ready to be filled with fluid).

In Fig.4.1 we show the results of experiments on ^{3}He-^{4}He mixtures in aerogel. The continous line is the phase diagram of the pure system. The circles represent experimental results in aerogel.

The experimental results show that in the presence of aerogel the coexistence line detaches from the normal-superfluid transition line, that now extends down to $T = 0$. Is it possible to interpret this result on the basis of the the Berker argument presented above?

The symmetry breaking first order transition has been converted to second order. Since the system is three dimensional, this behavior is either characteristic of a $O(1)$ model and disorder is strong, or of a $O(n)$, $n > 1$, model in weak disorder. Actually, the superfluid transition involves the breaking of a continous symmetry, therefore the latter seems to be more appropriate. Weak disorder seems to be at play also to explain the robustness of the coexistence transition. Since it resides completely inside the superfluid phase it does not involve any broken symmetry. It is a termally driven phase transition. The system which is undergoing the phase separation is a binary mixture, therefore $n = 1$ Ising-like variables are well suited to describe it. A three dimensional $O(1)$ system sustains termally driven first order phase transitions if disorder is weak. Therefore we gained an insight in the effects of weak quenched disorder on ^{3}He-^{4}He mixtures.

4.2 The Blume-Emery-Griffiths model

A simple model to describe superfluid ordering and phase separation is the Blume-Emery-Griffiths model (Blume, Emery and Griffiths (1971), Lajzerowicz and Sivardiere (1975), Sivardiere and Lajzerowicz (1975)) It captures the essential features of the system with a maybe crude but effective approximation. The continous superfluid order parameter is oversimplified using Ising spin variables: the phase of the wave function is not allowed to take any value on the unit circle but just the values ± 1. The ^{3}He atoms are described allowing the spin variables to assume the third value 0.

The most general Hamiltonian we can write for a spin-1 system (a system where the three values $\pm 1, 0$ are allowed) is

$$H_{BEG} = -J \sum_{<i,j>} \sigma_i \sigma_j + K \sum_{<i,j>} \sigma_i^2 \sigma_j^2 + D \sum_i \sigma_i^2 \quad ; \tag{4.2}$$

The D field is often called *anisotropy* since it prefers the 0 value of the spins than the ± 1 ones. The microscopic derivation of this Hamiltonian in the case of ^{3}He-^{4}He mixtures teaches us that $K = K_{33} + K_{44} - 2K_{34}$. K_{ij} is the microscopic interaction energy between atoms of ^{i}He and atoms of ^{j}He. Since it is due to their electronic structure and not to their isotopic species, $K \sim 0$ and (4.2) reduces to

$$H_{BC} = -J \sum_{<i,j>} \sigma_i \sigma_j + D \sum_i \sigma_i^2 \quad ; \tag{4.3}$$

which is the Blume-Capel (BC) Hamiltonian (Blume (1966), Capel (1966)) This will be the starting point for our analysis. The resulting phase diagram is presented in Figs. 4.2,4.3, showing great resemblance with the true pure system one (Fig.4.1) (Figs. 4.2,4.3 have been obtained using the techniques we will present in the next sections).

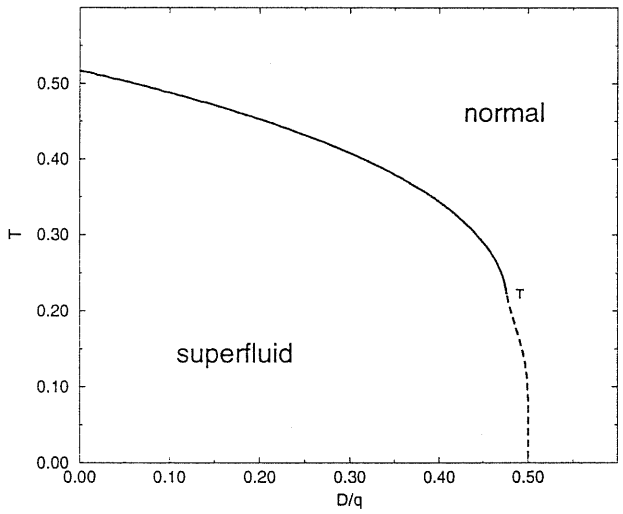

Figure 4.2: Temperature vs. anisotropy phase diagram of the BC model. Solid lines are second order phase transitions, dashed lines first order ones. T is the tricritical point.

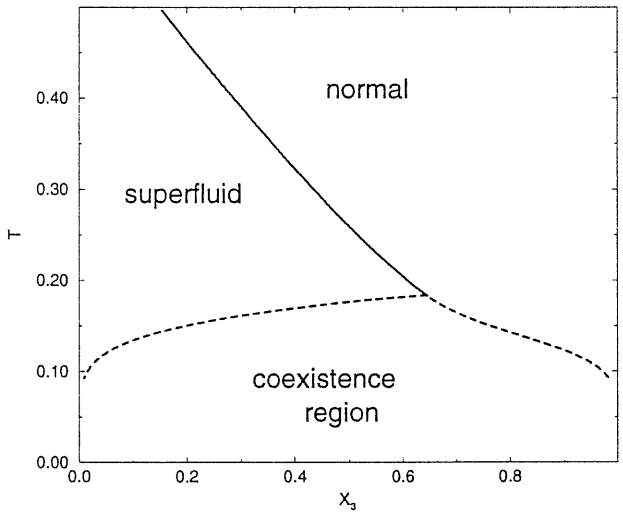

Figure 4.3: Temperature vs. ^{3}He concentration phase diagram of the BC model.

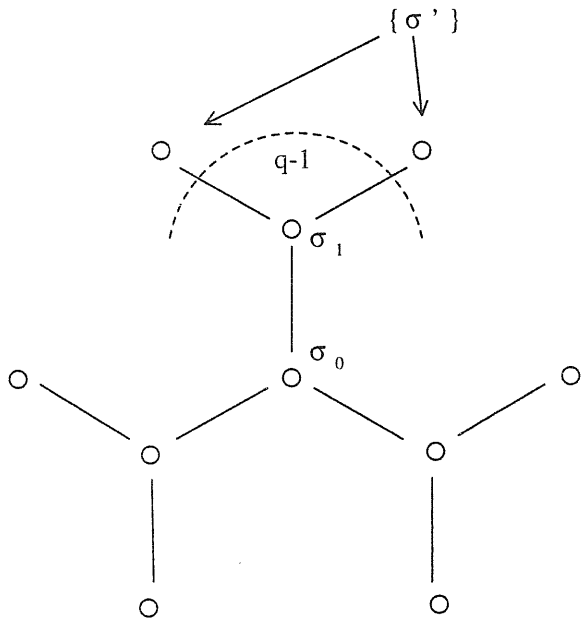

Figure 4.4: Sketch of a Cayley tree of coordination number $q = 3$

How do we introduce disorder in this scheme? Physically, the surface of the aerogel silica strands makes a difference between ^{3}He and ^{4}He, preferring the latter. The origin of this difference is an eminently quantum mechanical effect. In fact, altough the interaction energies between strands and He atoms depend on the electronic structure and not on the isotopic species (just as He-He interactions), ^{3}He is lighter and therefore has a greater zero point motion. Consequently it tends to be less localizable in space and on the strands in particular. We model this greater affinity of aerogel strands for ^{4}He playing with the anisotropy field D: it will be lower on the surface of the strands, higher in the bulk of the pores,

$$H = -J \sum_{<i,j>} \sigma_i \sigma_j + \sum_i D_i \sigma_i^2 \quad . \tag{4.4}$$

Since the aerogel strands are randomly distributed, D_i obeys a distribution probability such as

$$P(D_i) = (1-p)\, \delta(D_i - D) \; + \; + p\, \delta(D_i - D + \epsilon) \tag{4.5}$$

where p is the probability of a site to be on the surface of a strand and ϵ is a parameter tuning the different affinity of ^{3}He and ^{4}He for silica.

4.3 Formal solution of the model on the Bethe lattice

In order to analyze the system we work on a Bethe lattice with coordination number $q = 4$ (Fig.4.4).

We can then use the Baxter approach (Baxter (1982)). The partition function for an n-generation Cayley tree (we remember that the Bethe lattice is the thermodynamic limit, $n \to \infty$, of the Cayley tree).

$$Z_n = \sum_{\{\sigma_0\}} \exp(-\beta D_0 {\sigma_0}^2) \prod_{i=1}^{q} g_n^{(i)}(\sigma_0) \tag{4.6}$$

with

$$g_n^{(i)}(\sigma_0) = \sum_{\{\sigma'\},\{\sigma_1\}} \exp\left[\beta\left(J \sum_{<j,l>} \sigma_j'\sigma_l' - \sum_j D_j {\sigma_j'}^2 + J\sigma_0\sigma_i - D_i\sigma_i^2 + J\sigma_i \sum_{<1,j>} \sigma_j'\right)\right]. \tag{4.7}$$

g_n satisfies the recurrence relation

$$g_{n+1}(\sigma) = \sum_{\sigma_1} \exp\left[-\beta\left(D_1\sigma_1^2 - J\sigma_1\sigma\right)\right] \prod_{j=1}^{q-1} g_n^{(j)}(\sigma_1). \tag{4.8}$$

The order parameters can be found as

$$< \sigma >_n = \frac{\sum_{\{\sigma\}} \sigma \exp(-\beta D_0\sigma^2) \prod_{j=1}^{q} g_n^{(j)}(\sigma)}{Z_n}, \tag{4.9}$$

and

$$< \sigma^2 >_n = \frac{\sum_{\{\sigma\}} \sigma^2 \exp(-\beta D_0\sigma^2) \prod_{j=1}^{q} g_n^{(j)}(\sigma)}{Z_n}. \tag{4.10}$$

We can now recast everything by just a simple normalization. Upon defining

$$x_n = \frac{g_n(-1)}{g_n(+1)}, \quad z_n = \frac{g_n(0)}{g_n(+1)} \tag{4.11}$$

obtaining the following recursion relations for x_n and z_n:

$$x_{n+1} = \frac{e^{-\beta J} + e^{J} \prod_{j=1}^{q-1} x_n^{(j)} + e^{\beta D_1} \prod_{j=1}^{q-1} z_n^{(j)}}{e^{\beta J} + e^{-\beta J} \prod_{j=1}^{q-1} x_n^{(j)} + e^{\beta D_1} \prod_{j=1}^{q-1} z_n^{(j)}} \tag{4.12}$$

and

$$z_{n+1} = \frac{1 + \prod_{j=1}^{q-1} x_n^{(j)} + e^{\beta D_1} \prod_{j=1}^{q-1} z_n^{(j)}}{1 + \prod_{j=1}^{q-1} x_n^{(j)} + e^{\beta D_1} \prod_{j=1}^{q-1} z_n^{(j)}} \tag{4.13}$$

Then we can obtain expressions for the order parameters

$$< \sigma >_n = \frac{\prod_{i=1}^{q} x_n^{(i)} - 1}{\prod_{i=1}^{q} x_n^{(i)} + 1 + e^{\beta D_0} \prod_{i=1}^{q} z_n^{(i)}} \tag{4.14}$$

and

$$< \sigma^2 >_n = \frac{\prod_{i=1}^{q} x_n^{(i)} + 1}{\prod_{i=1}^{q} x_n^{(i)} + 1 + e^{\beta D_0} \prod_{i=1}^{q} z_n^{(i)}} \tag{4.15}$$

What about the free energy?

Since a Cayley tree has a number of *surface* sites that is 1/2 of the total number of sites and we are interested in the bulk behaviour of the system, we must get rid of them. We can use the formula (Gujrati (1995))

$$f = -\frac{1}{q\beta}\lim_{n\to\infty}[\ln Z_n - \sum_{i=1}^{q-1}\ln Z_{n-1}^{(i)}] \tag{4.16}$$

which, using (4.12),(4.13), yelds

$$f = -\frac{1}{\beta}\{\ln[e^{-\beta D_0-\beta J}\prod_{i=1}^{q-1}x^{(i)}+e^{-\beta D_0+\beta J}+\prod_{i=1}^{q-1}z^{(i)}]+\frac{q-2}{q}\ln[e^{-\beta D_0}\prod_{i=1}^{q}x^{(i)}+e^{-\beta D_0}+\prod_{i=1}^{q}z^{(i)}]\} \tag{4.17}$$

where $x^{(i)}$ and $z^{(i)}$ are the fixed points of the recurrence relations (4.12) and (4.13). Expression (4.17) gives the *bulk* free energy per site.

This formula for the free energy is at variance with the generalization to spin-1 systems of the one presented in (Bruinsma (1984)) when dealing with the Random Field Ising model on the Bethe lattice. Actually, the simple generalization of Bruinsma's formula gives the wrong results when tested for very negative values of D, where the system reduces to a Ising model whereas (4.16) turns out to be correct, and it is also correct for the pure system when compared with the mean-field pair approximation (which is exact on the Bethe lattice).

Before examining the behavior of the disordered system, we use the previous relations to obtain the phase diagram for the pure system (Figs.4.2,4.3), that is found to be in full agreement with the same behavior as found in the pair (Bethe) approximation on a square lattice. Therefore we go on confident in our expressions for the order parameters and the free energy.

The preceeding expressions are valid for a given realization of disorder. We want to obtain the average of the order parameters and of the free energy with respect of the disorder, so that we should in principle describe the evolution of the probability distribution $P(x_n, z_n)$ (Bruinsma (1984)). Given the expressions (4.12) and (4.13) we obtain

$$\begin{aligned} P(x_{n+1}, z_{n+1}) &= \int \delta(x_{n+1} - k(\{x_n^{(i)}\},\{z_n^{(i)}\},D))\delta(z_{n+1} - h(\{x_n^{(i)}\},\{z_n^{(i)}\},D)) \\ &\quad \prod_{i=1}^{q-1} P_i(x_n, z_n)P(D)\prod_{i=1}^{q-1}(dx_n^{(i)}dz_n^{(i)})dD \end{aligned} \tag{4.18}$$

where the functions k and h are the r.h.s of Eqs. (4.12) and (4.13) respectively.

We look at the properties of the solution when $n \to \infty$. Then the high order phase ($< \sigma > \sim 1$) is characterized by values of x close to 0, and the low order one ($< \sigma > \sim 0$) by values of x close to 1. This helps us in the choice of the initial probability distribution for (4.18). In order to find the high order fixed point we choose a probability distribution

with a mean value close to $(x = 0, z = 0)$, and close to $(x = 1, z = 1)$ for the low order fixed point. In any case $0 < x < 1$, that is $< \sigma > \geq 0$. Then we use the method explained in (Bruinsma (1984)), where only a $P(x)$ was considered: we generate a two dimensional pool of points distributed according to the initial probability distribution. Using (4.18) we generate a new pool of (x, z) pairs, and so on until convergence is achieved (convergence is defined in terms of the stability upon iteration of the mean values and of the variances of the pool).

Using this method both first and second order phase transitions can be found. First order phase transitions are obtained looking at the free energy difference between the low and high order phase: a change of sign of this difference is a signature of a phase transition. Second order phase transitions are more difficult to find with this recipe. In fact they can be detected looking at the point where the magnetization (4.14) goes to 0. Due to numerical precision, $< \sigma >$ is considered zero if its value is below a given threshold σ_c. Due to strong disorder induced fluctuations, the value of the threshold is strictly related to the dimensions of the pool. We used pools ranging from 50000 to 150000 points, allowing us to unambigously detect a second order phase transtion with a threshold value $\sigma_c = 0.01$. We checked the stability of the second order line determined in this way letting the threshold σ_c vary between 0.01 and 0.1. Variations of the positions of the transition points are less than 5%. Moreover the upper part of the second order transition line, high temperature and low ^{3}He concentration $1 - < \sigma^2 >$, goes toward the pure model.

4.4 Discussion of the results

We follow numerically (4.18) on a Bethe lattice with coordination number $q = 4$. We take $\epsilon = 2$ and $p = 0.1, 0.8$.

When $p = 0.1$ (low aerogel concentration, Fig.4.5), the system exhibits a behavior similar to the one of the pure system. The main difference is that the normal-superfluid coexistence line does not split the system in two isotopic pure phases at $T = 0$. Whereas the superfluid side of the transition still corresponds to a pure ^{4}He phase, the normal side is not a pure ^{3}He phase like in the pure model ($p = 0$). A closer scrutiny of the phase diagram reveals that the ^{3}He concentration at the $T = 0$ on the normal side of the phase transition is close to $1 - p$. This result can be interpreted as an aerogel effect. The *bulk* system (that is the part of the system inside the pores of the aerogel) actually splits in a superfluid pure ^{4}He phase and in a pure ^{3}He phase, but the latter has to be properly $1 - p$ weighted in order to take into account the presence of ^{4}He atoms in a normal state that are covering the silica strand surface. The fact that the ^{4}He atoms on the strand surface are in a normal state can be understood if we remember that in our model (4.4) there is no correlation among the sites: we are not properly looking at an aerogel, which is a connected structure, but

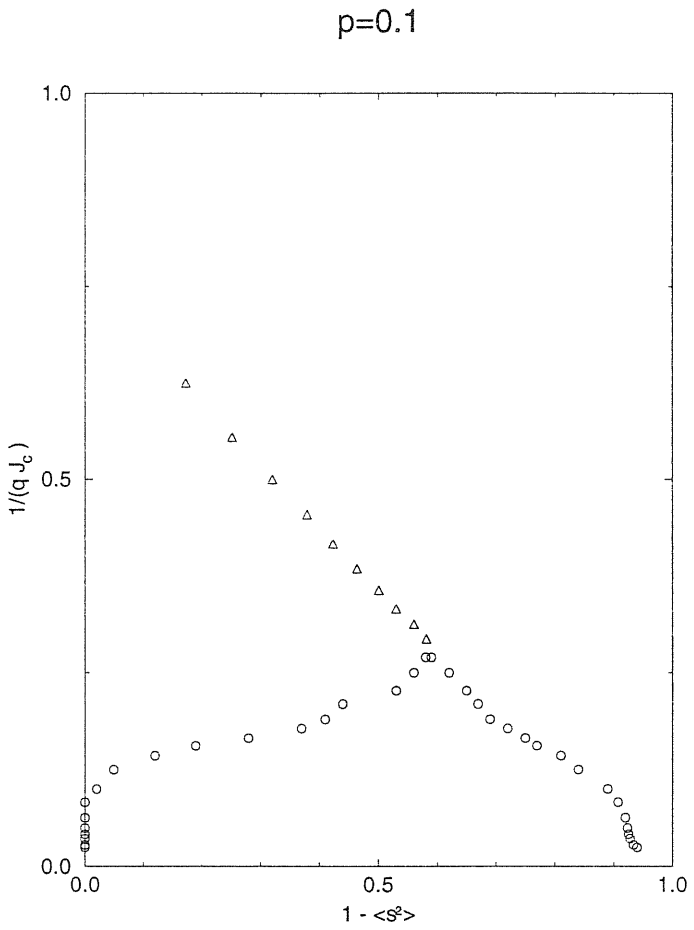

Figure 4.5: Phase diagram of the BC model on the Bethe lattice for $p = 0.1$. Triangles are for second order phase transitions, circles are for first order ones.

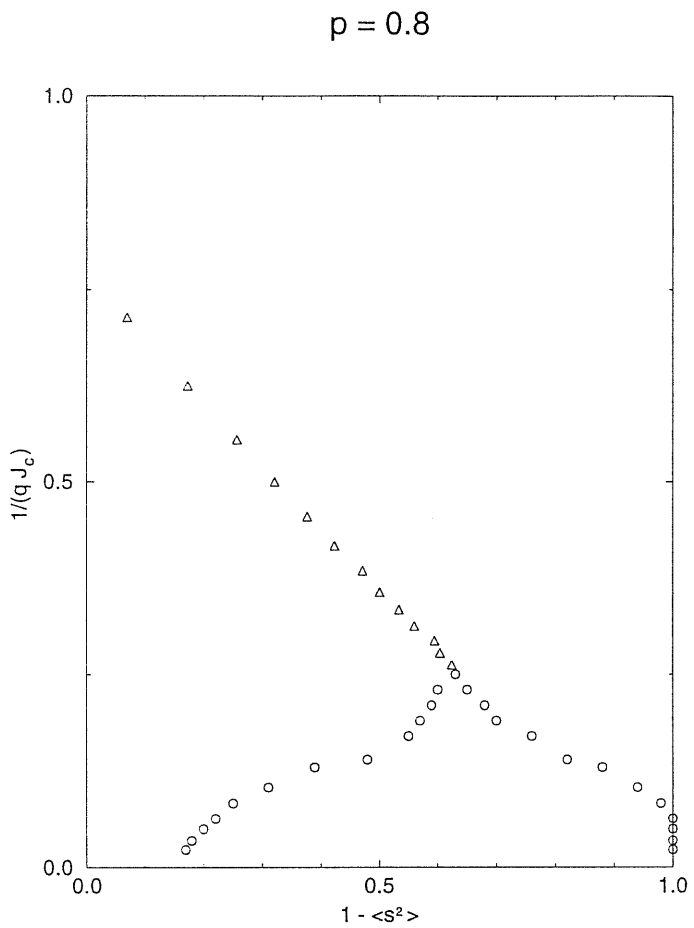

Figure 4.6: Phase diagram of the BC model on the Bethe lattice for $p = 0.8$. Triangles are for second order phase transitions, circles are for first order ones.

at a random distribution of *pores* with concentration p. When p is below the percolation threshold (in our case $p_c = \frac{1}{q-1} = \frac{1}{3}$) there is not an infinite cluster, then there cannot be a phase transition related to the atoms on the surface of the strands.

When $p = 0.8$ (high aerogel concentration, Fig.4.6), the system again exhibits a behaviour which is very similar to that of the pure system. In this case the coexistence region extends (at $T = 0$) from the pure ^{3}He normal phase to a mixture with a ^{3}He concentration close to $1 - p = 0.2$. In this case the result can be interpreted as if the strand surface was covered by ^{4}He atoms in a superfluid state. Now the silica concentration is higher than the percolation threshold, so that there is an infinite cluster spanning the lattice. This cluster can sustain a superfluid phase.

The Bethe lattice results obtained for the two extreme cases $p = 0.1$ and $p = 0.8$ show that the tricritical point has some robustness. At intermediate values of p, in particular near the critical percolation threshold, there is some evidence that structures of the phase diagram similar to mean field can also be found.

Real aerogel forms connected structures, so that (4.4) with $p < p_c$ or $1 - p < p_c$ will never be a good model for aerogels. The behavior of the true system should be much closer to the Bethe lattice one when $p_c < p < 1 - p_c$, with both the silica strands and the bulk of the lattice forming connected percolating structures. Regretfully, our method, with the dimensions of the pools we considered, is not able to extend to that regions. In fact it becomes much more difficult to doubtlessly identify both first and second order phase transitions. Whereas this is mainly due poor statistics, we can anyway learn something. In fact it means that the attractive points of the recurrence we numerically follow are "weak" (very likely their basin of attraction is quite small). We interpret this result as a "weakening" of the phase transitions of the system, as we should expect in the presence of conversion or elimination of phase transitions. On the contrary, when $p < p_c$ or $p > 1-p_c$ we find robust phase transitions. Does this robustness teach us anything? The Bethe lattice is a structure where thermodynamic quantities are behave in a mean-field fashion, yet, working on it, we could deal with correlations in disorder. The outcome of the calculations is that if the distribution of disorder has some topological properties, such as percolative effects, they can manifest themselves making it possible for the system to sustain phase transitions. As we previously pointed out in Chapter 2, when percolative effects are at play, naïve coarse graining arguments can fail, since features such as percolation are robust under renormalization steps. They are not simply blurred in such a way that at last the coarse grained region is subject to the Central Limit Theorem. This is is one of the limits of arguments such as the Imry-Ma and Berker ones. Since anyway the Bethe lattice is somewhat an infinite dimensional structure, and we know that phase transitions get more robust as the dimension increases, it would be extremely interesting to understand the consequence of the presence of percolative properties in the disorder distribution also for low dimensionalities.

5 Appendix 1: $1+\epsilon$ expansion on hierarchical lattices

In Chapter 2 we anticipated that some analytical result for the behavior of polymers in disorderd media can be obtained through a $1+\epsilon$ expansion on hierarchical lattices. In this Appendix we come back to this problem, reformulating it at variance with (Derrida and Griffiths (1989)) to show that the approach can be extended to distributions different from Gaussians. In particular we are interested in distributions with infinite second and/or first moments. For analytical reasons that will be clear in what follows, we will concentrate on Levy distributions $L_\mu(x)$ defined through their Fourier Transform (FT)

$$\tilde{L_\mu}(k) = \int_{-\infty}^{+\infty} e^{-ikx} L_\mu(x) dx = e^{-|k|^\mu} \quad , \tag{5.1}$$

If $\mu = 2$ then we recover the Gaussian distribution, else, when $0 < \mu < 2$, these distributions have a power law behavior at infinity

$$L_\mu(x) \sim |x|^{-1-\mu} \qquad |x| \to \infty \ . \tag{5.2}$$

A nice property of Levy distributions is that they are stable under convolution (from which their other name of *stable* distributions), that is,

$$L_\mu(x) * L_\mu(x) = 2^{-\frac{1}{\mu}} L_\mu(2^{-\frac{1}{\mu}} x) \tag{5.3}$$

as it is immediately evident from their FT definition (5.1) remembering that the FT of a convolution is is the product of FTs and that exponentials are stable under the product.

Equation (5.3) can be straightforwardly extended to the convolution of N distributions. leading to

$$L_\mu(x) * ... * L_\mu(x) = N^{-\frac{1}{\mu}} L_\mu(N^{-\frac{1}{\mu}} x) \tag{5.4}$$

Eq.(5.4) can be interpreted as the exact solution for 1−dimensional hierarchical lattices. We concentrate on the half-width σ of the distribution which is defined as the width where the distribution has a value half of that in the origin: for Gaussians it is easy to show that it is proportional to the variance, therefore it scales in the same way with the length of

the lattice; for Levy distributions with $\mu < 2$ the variance is infinite but the half-width is defined with scaling properties. Doubling the length of the lattice in (5.4) the half width scales as $2^{\frac{1}{\mu}}$. Therefore the exponent $\omega = \frac{1}{\mu}$ (if $\mu = 2$ Levy distributions become Gaussians and we recover the usual Central Limit Theorem $\omega = \frac{1}{2}$).

We now move on to the analysis of the $1+\epsilon$ expansion. For the reader's convenience we recall the general approach on hierachical lattices as in Fig. 2.3 with b sides ($b = 2$ and $b = 4$ respctively in Fig. 2.3). The fractal dimension of the lattice is related to b by the relation

$$D_f = \log_2(2b) \tag{5.5}$$

inverting which we have

$$b = 2^{D_f - 1} \tag{5.6}$$

If $D_f = 1+\epsilon$ then $b = 1+\epsilon$ (multiplication constants have been absorbed in ϵ).

The hierarchical nature of the lattice means that the ground state energy $E^{(n+1)}$ of a lattice of generation $(n+1)$ can be written as

$$E^{(n+1)} = min(E_1^{(n)} + E_2^{(n)}, E_3^{(n)} + E_4^{(n)}, ..., E_{2b-1}^{(n)} + E_{2b}^{(n)}) \ ; \tag{5.7}$$

where the $E_i^{(n)}$ are the ground state energies of lattices of generation n. As these are independent random variables, (5.7) yelds a recursion relation for the probability distribution $P_n(E^{(n)})$:

$$Q_n(x) = P_n(x) * P_n(x) \tag{5.8}$$

$$\int_x^{+\infty} P_{n+1}(y)dy = \left[\int_x^{+\infty} Q_n(y)dy\right]^b \ . \tag{5.9}$$

In order to write the expansion around one dimension we must write $b = 1+\epsilon$ and an expression for $P_n(x)$ around the one dimensional result

$$P_n(x) = \frac{1}{\delta_n} L_\mu(\frac{x-\gamma_n}{\delta_n}) \left[1 + \epsilon\phi_n(\frac{x-\gamma_n}{\delta_n}) + O(\epsilon^2)\right] \ . \tag{5.10}$$

For $P_n(x)$ to be normalized ϕ_n has to satisfy

$$\int_{-\infty}^{+\infty} L_\mu(x)\phi_n(x)dx = 0 \ . \tag{5.11}$$

By means of (5.8) and of (5.9), and ignoring terms of order $O(\epsilon^2)$, we obtain the expression

$$\begin{aligned} P_{n+1}(x) &= \frac{1}{2^{\frac{1}{\mu}}\delta_n} L_\mu(\frac{x-2\gamma_n}{2^{\frac{1}{\mu}}\delta_n}) \left[1 + \epsilon + \epsilon F(\frac{x-2\gamma_n}{2^{\frac{1}{\mu}}\delta_n})\right] \\ &+ 2\epsilon \left[\frac{1}{\delta_n} L_\mu(\frac{x-\gamma_n}{\delta_n})\right] * \left[\frac{1}{\delta_n} L_\mu(\frac{x-\gamma_n}{\delta_n})\phi_n(\frac{x-\gamma_n}{\delta_n})\right] \ , \end{aligned} \tag{5.12}$$

where F is defined as

$$F(x) = \ln \left[\int_x^{+\infty} L_\mu(y) dy \right] \quad . \tag{5.13}$$

This equation is more general than the one reported in (Derrida and Griffiths (1989)). but poses some new problems to solve it.

The non trivial part of (5.12) comes from the last term in its *r.h.s.* We propose a way out through the following eigenvalue equation

$$2 \left[\frac{1}{\delta_n} L_\mu(\frac{x-\gamma_n}{\delta_n}) \right] * \left[\frac{1}{\delta_n} L_\mu(\frac{x-\gamma_n}{\delta_n}) \phi_n(\frac{x-\gamma_n}{\delta_n}) \right] = \lambda_n \frac{1}{2^{\frac{1}{\mu}} \delta_n} L_\mu(\frac{x-2\gamma_n}{2^{\frac{1}{\mu}} \delta_n}) \phi_n(\frac{x-2\gamma_n}{2^{\frac{1}{\mu}} \delta_n}) \tag{5.14}$$

whose solutions are the functions of the form

$$\phi_n(x) = (-1)^n L_\mu^{-1}(x) \frac{d^n}{dx^n} L_\mu(x) \quad , \tag{5.15}$$

and the corresponding eigenvalues are

$$\lambda_n = 2^{1-\frac{n}{\mu}} \quad . \tag{5.16}$$

If $\mu = 2$ L_μ is a Gaussian distribution, and the $\{\phi_n\}$ functions are the Hermite polynomials and substitution in (5.12) gives back the results of (Derrida and Griffiths (1989)) . If $0 < \mu < 2$ (5.15) are new non-polynomial functions.

Therefore we can at last write the equation

$$P_{n+1}(x) = \frac{1}{2^{\frac{1}{\mu}} \delta_n} L_\mu(\frac{x-2\gamma_n}{2^{\frac{1}{\mu}} \delta_n}) \left[1 + \epsilon + \epsilon F(\frac{x-2\gamma_n}{2^{\frac{1}{\mu}} \delta_n}) + \epsilon \lambda_n \phi_n(\frac{x-2\gamma_n}{2^{\frac{1}{\mu}} \delta_n}) \right] \quad , \tag{5.17}$$

and then go on with the expansion. In this Appendix we showed that exploring the behavior of the systems with non-Gaussian distributions is feasible as long as the distributions are stable under convolution.

6 Appendix 2: A possible relation between the Bak -Sneppen model and random walks

Recently Maslov, Paczuski and Bak (Maslov et al. (1994), Paczuski, Maslov and Bak (1996)a) thoroughly investigated analytically and numerically the properties of some self-organized critical (SOC) models, among which the celebrated Bak-Sneppen (BS) model of biological evolution (Bak and Sneppen (1993)). They proposed and checked numerically a simple scaling relation between the "lifetime" exponents for the first and all returns of activity on the same site

$$\tau_f + \tau_a = 2 \ . \tag{6.1}$$

They verified this result simulating the BS branching process, on which the BS model can be mapped exactly (Paczuski, Maslov and Bak (1996)b). From the computational point of view, the great merit of the BS branching process is that it does not show any finite size effects: each site of an avalanche is kept in memory as long as it is active (its fitness is below the threshold of the model), eliminated otherwise. An avalanche stops when there are no more sites left in the computer memory. Their results are nicely consistent with (6.1), being $\tau_f = 1.58(2)$ and $\tau_a = 0.42(2)$ in one dimension, $\tau_f = 1.28(3)$ and $\tau_a = 0.70(3)$ in two dimensions. Moreover they claim that just two exponents are enough to describe all the physical properties of the model, namely τ_a (or the fractal dimension of the avalanches, $D = d/\tau_a$) and the exponent τ of the avalanche size distribution ($P_{ava}(t) \sim t^{-\tau}$, $\tau = 1.07(1)$ in 1−d, $\tau = 1.25(1)$ in 2−d (Paczuski et al. (1996)a))

First of all, we observe that the BS branching process collects return times within a single avalanche. If we define the intrinsic first return probability $P_f^{(i)}(t)$ for avalanches of duration greater than t, then the first return probability $P_f^{(m)}(t)$, measured in (Maslov et al. (1994), Paczuski et al. (1996)a) can be expressed as

$$P_f^m(t) = P_f^i(t) \cdot \int_t^\infty P_{ava}(t')dt' \ , \tag{6.2}$$

where the integral in the *r.h.s* represents the probability of avalanches of duration greater

than t. From (6.2) it immediately follows that

$$P_f^{(i)}(t) \sim t^{-\tau_f^{(i)}} \quad , \tag{6.3}$$

with

$$\tau_f^{(i)} = \tau_f^{(m)} - \tau + 1 \quad . \tag{6.4}$$

From the values of $\tau_f^{(m)}$ and τ quoted in (Maslov et al. (1994), Paczuski et al. (1996)a). we get $\tau_f^{(i)} = 1.51(3)$ and $\tau_f^{(i)} = 1.03(4)$ in 1−d and 2−d respectively. These exponents suggest that the intrinsic first return probability behaves asymptotically as that of a random walk (Montroll and Weiss (1965)).

We therefore conjecture that the only non trivial exponent of the BS branching process is the avalanche exponent τ, and, using (6.1),

$$\tau_a = \frac{2+d}{2} - \tau \quad . \tag{6.5}$$

7 Aknowledgments

There comes a time in life when we look at ourselves and realize that there is much more of other people to us than we could ever have imagined. And I think that I ought them all my gratitude. Yet, of course there are people with whom I feel much more indebted, and I don't want to miss this opportunity to tell them.

I'm trying to be a physicist, and only future knows if I will succeed. But the roots of my achievements can be found in my passion for physics that has been fed mainly by three people. Carla Buzano, whose patience and frienship didn't make me feel like a stranger in a strange land, deserves my first thank. Erio Tosatti, who taught me to learn physics from physics (even if almost everything we did together had much more mathematics than I expected: but I like and liked it a lot!). Amos Maritan, a good friend and teacher, led me here and gave me a mouthfull of physics (sometimes much more than I could chew), with so many different tastes that I think I will never get bored.

I am very gratefull also to all those people with whom I shared some good moments and a little bit of work: Flavio Seno, Jayanth Banavar, Marek (Caldarelli) Cieplak, Laura Bonesi, Guido, Michele, Claudio, Nicola Manini, Attilio Stella, Achille Giacometti, Lucian, Michael Swift, Stefano Galluccio.

Thanks to Fabia, Andrea, Riccardo and of course Sabrina for their smiling attitude while working.

After due worshipping, let me skip to the salt of my life.

I spent three years in Trieste, a long period that rolled away much faster than I expected, so that in some way I am still not prepared to waive goodbye to all the friends I met here.

I don't want to pour honey on these pages, therefore I will try to be as exhaustive and short as possible remembering most of them. I will never forget Sandro and Francesca, the early birds; Leonardo, who maybe at last will find what he is looking for; Claudio, maybe one day you will publish it (you know what I mean).

How much physics passed by in room 27? How much of it could eventually go safely (or I should say smoothly?) away? Who knows, and, after all, who cares? Laughing and joking

we had a great time, and I think that the non-serious spirit with which we dedicated most days to physics is a precious lesson I learned from GCalda and Michele.

How should I describe the cheerful situation comedy "Casa Bondel"? I think I will miss a lot Njofra, Gabriele, Marco and Gabriele back again. Three years are not enough to appreciate you.

Last but not least, Stefano, who welcomed me in Trieste; we ended up much *closer* than an Asti-Torino train trip.

Of course I would have had a much harder time without all the people far in Torino supporting me. My dearest company, Elena and Carlo, who always encouraged me to go further on. And Flavio, Stefano. Luisa, Mario.

Usually what we say last is what is remembered, therefore I saved the last lines for those people who really made me from nothing, giving me their love and care, their unextinguishable support and encouragement. My parents and my unspeakable brother. Thank you mom, dad and Riccardo.

Bibliography

Ala-Nissila, T., Hjelt, T., Kosterlitz, J. and Venäläinen, O.: (1993), *J. Stat. Phys.* **72**, 207.

Ambegaokar, V., Halperin, B. and Langer, J.: (1971), *Phys. Rev. B* 4, 2612.

Bak, P. and Sneppen, K.: (1993), *Phys. Rev. Lett.* **71**, 4083.

Bak, P., Tang, C. and Wiesenfeld, K.: (1987), *Phys. Rev. Lett.* **59**, 381.

Bak, P., Tang, C. and Wiesenfeld, K.: (1988), *Phys. Rev. A* **38**, 364.

Balents, L. and Kardar, M.: (1992), *J. Stat. Phys.* **67**, 1.

Barabasi, L. and Stanley, G.: (1995), *Fractal concepts in the interface growth*, Cambridge University Press, Cambridge.

Baxter, R.: (1982), *Exactly Solved models in Statistical Mechanics*, Academic Press, London.

Ben-Hur, A. and Biham, O.: (1996), *Phys. Rev. E* **53**, R1317.

Berker, A. N.: (1993), *Physica A* **194**, 72.

Berker, A. and Ostlund, S.: (1989), *J. Phys. C* **12**, 4961.

Berman, D., Orr, B., Jaeger, H. and Goldman, A.: (1986), *Phys. Rev. B* **33**, 4301.

Bhat, R. and Lee, P.: (1982), *Phys. Rev. Lett.* **48**, 344.

Blume, M.: (1966), *Phys. Rev.* **141**, 517.

Blume, M., Emery, V. and Griffiths, R. B.: (1971), *Phys. Rev. A* 4, 1071.

Brezinski, C.: (1971), *C. R. Acad. Sci. Paris* **A273**, 427.

Bricmont, J. and Kupiainen, A.: (1987), *Phys. Rev. Lett.* **59**, 1829.

Bruinsma, R.: (1984), *Phys. Rev. B* **30**, 289.

Caldarelli, G., Tebaldi, C. and Stella, A.: (1996), *Phys. Rev. Lett.* **76**, 4983.

Capel, H.: (1966), *Physica* **32**, 966.

Cardy, J. and Sugar, R.: (1980), *J. Phys. A* **13**, L423.

Carlson, J. and Langer, J.: (1989), *Phys. Rev. Lett.* **62**, 2632.

Chan, M., Mulders, N. and Reppy, J.: (1996), *Physics Today (August)* .

Chau, H., Mak, L. and Kwok, P.: (1995), *Physica A* **215**, 431.

Chen, K., Bak, P. and Jensen, M.: (1990), *Phys. Lett. A* **149**, 207.

Cieplak, M., Maritan, A. and Banavar, J.: (1994)a, *Phys. Rev. Lett.* **72**, 2320.

Cieplak, M., Maritan, A. and Banavar, J.: (1994)b, *J. Phys. A* **27**, L765.

Cieplak, M., Maritan, A. and Banavar, J.: (1996), *Phys. Rev. Lett.* **72**, 3754.

Cieplak, M., Maritan, A., Swift, M., Bhattacharaya, A., Stella, A. and Banavar, J.: (1995). *J. Phys. A* **28**, 5693.

Cieplak, M. and Robbins, M.: (1988), *Phys. Rev. Lett.* **60**, 2042.

Dasgupta, C. and Ma, S.: (1980), *Phys. Rev. B* **22**, 1305.

de Boer, J., Derrida, B., Flyvbjerg, H., Jackson, A. and Wettig, T.: (1994), *Phys. Rev. Lett.* **73**, 906.

de Boer, J., Jackson, A. and Wettig, T.: (1995), *Phys. Rev. E* **51**, 1059.

Derrida, B. and Griffiths, R.: (1989), *Europhys. Lett.* **8**, 111.

Edwards, S. and Anderson, P.: (1975), *J. Phys. F* **5**, 965.

Edwards, S. and Wilkinson, D.: (1982), *Proc. Roy. Soc. London A* **381**, 17.

Eldredge, N. and Gould, S.: (1988), *Nature (London)* **332**, 211.

Elena, S., Cooper, V. and Lenski, R.: (1996), *Science* **272**, 1802.

Essam, J., De'Bell, K., Adler, J. and Bhatti, F.: (1986), *Phys. Rev. B* **33**, 1982.

Essam, J., Guttmann, A. and De'Bell, K.: (1988), *J. Phys. A* **21**, 3815.

Fisher, D.: (1992), *Phys. Rev. Lett.* **69**, 534.

Fisher, D. and Huse, D.: (1991), *Phys. Rev. B* **43**, 10728.

Fishman, S. and Aharony, A.: (1976), *J. Phys. C* **12**, L729.

Flyvbjerg, H., Sneppen, K. and Bak, P.: (1993), *Phys. Rev. Lett.* **71**, 4087.

Forster, D., Nelson, D. and Stephen, M.: (1977), *Phys. Rev. A* **16**, 732.

Gardiner, C.: (1985), *Handbook of stochastic methods for physics, chemistry, and the natural sciences*, Springer series in synergetics 13.

Gould, S.: (1977), *Paleobiology* **3**, 135.

Grassberger, P.: (1989), *J. Phys. A* **22**, 3673.

Grassberger, P.: (1995), *Phys. Lett. A* **200**, 277.

Gujrati, P.: (1995), *Phys. Rev. Lett.* **74**, 809.

Halpin-Healy, T. and Zhang, Y.: (1995), *Physics Reports* **254**, 215.

Henkel, M. and Schütz, G.: (1988), *J. Phys. A* **21**, 2617.

Higashi, M. and Nakajima, H.: (1995), *Math. Biosci.* **130**, 99.

Hirsch, J. and Jose, J.: (1980), *Phys. Rev. B* **22**, 5339.

Huse, D. and Henley, C.: (1985), *Phys. Rev. Lett.* **54**, 2708.

Huse, D., Henley, C. and Fisher, D.: (1985), *Phys. Rev. Lett.* **55**, 2924.

Imry, Y. and Ma, S. K.: (1975), *Phys. Rev. Lett.* **35**, 1399.

Kardar, M.: (1985), *Phys. Rev. Lett.* **55**, 2923.

Kardar, M.: (1987), *Nucl. Phys. B* **290**, 582.

Kardar, M., Parisi, G. and Zhang, Y.: (1986), *Phys. Rev. Lett.* **56**, 889.

Kardar, M. and Zhang, Y.: (1987), *Phys. Rev. Lett.* **58**, 2087.

Katz, A. and Thompson, A.: (1986), *Phys. Rev. B* **34**, 8179.

Kinzel, W. and Yeomans, J.: (1981), *J. Phys. A* **14**, L163.

Lajzerowicz, J. and Sivardiere, J.: (1975), *Phys. Rev. A* **11**, 2079.

Lebedev, N. and Zhang, Y.: (1995), *J. Phys. A* **28**, L1.

Marconi, U. M. B. and Zhang, Y.: (1990), *J. Stat. Phys.* **61**, 885.

Maritan, A., Colaiori, F., Flammini, A., Cieplak, M. and Banavar, J.: (1996), *Science* **272**, 984.

Maslov, S., Paczuski, M. and Bak, P.: (1994), *Phys. Rev. Lett.* **73**, 2162.

Montroll, E. and Weiss, G.: (1965), *J. Math. Phys.* **6**, 167.

Moore, M., Blum, T., Doherty, J., Marsili, M., Bouchaud, J. and Claudin, P.: (1995), *Phys. Rev. Lett.* **74**, 4257.

Newman, C. and Stein, D.: (1994), *Phys. Rev. Lett.* **72**, 2286.

Newman, M. and Roberts, B.: (1995), *Proc. Roy. Soc. Lond. B* **260**, 31.

Paczuski, M., Maslov, S. and Bak, P.: (1996)a, *Phys. Rev. E* **53**, 414.

Paczuski, M., Maslov, S. and Bak, P.: (1996)b, *Europhys. Lett.* **27**, 97.

Parisi, G. and Sourlas, N.: (1979), *Phys. Rev. Lett.* **43**, 744.

Parisi, G. and Sourlas, N.: (1982), *Nucl. Phys. B* **206**, 321.

Peliti, L.: (1985), *Lectures given at the NATO ASI on Physics of Biomaterials: Fluctuations, Self-Assembly and Evolution.*

Petri, A., Paparo, G., Vespignani, A., Alippi, A. and Costantini, M.: (1994), *Phys. Rev. Lett.* **73**, 3423.

Pietronero, L., Vespignani, A. and Zapperi, S.: (1994), *Phys. Rev. Lett.* **72**, 1970.

Raup, M.: (1986), *Science* **251**, 1530.

Rinaldo, A., Rodriguez-Iturbe, I., Rigon, R., Ijjasz-Vasquez, E. and Bras, R.: (1993), *Phys. Rev. Lett.* **70**, 822.

Rios, P. D. L., Caldarelli, G., Maritan, A. and Seno, F.: (1996), *Phys. Rev. E* **53**, R2029.

Roux, S., Hansen, A. and Guyon, E.: (1987), *J. de Phys.* **48**, 2125.

Roux, S., Hansen, A. and Hinrichsen, E.: (1991), *J. Phys. A* **24**, L295.

Roux, S. and Zhang, Y.: (1996), *J. Phys. I (Paris)* **6**, 385.

Sherrington, D. and Kirkpatrick, S.: (1975), *Phys. Rev. Lett.* **35**, 1972.

Sivardiere, J. and Lajzerowicz, J.: (1975), *Phys. Rev. A* **11**, 2090.

Sneppen, K.: (1992), *Phys. Rev. Lett.* **69**, 3539.

Sneppen, K.: (1993), *Phys. Rev. Lett.* **71**, 101.

Stauffer, D. and Aharony, A.: (1992), *Introduction to Percolation Theory, 2nd Edition*, Taylor & Francis, London.

Vendruscolo, M., Rios, P. D. L. and Bonesi, L.: (1996), *Phys. Rev. E* .

Vespignani, A., Zapperi, S. and Pietronero, L.: (1995), *Phys. Rev. E* **51**, 1711.

Wilkinson, D. and Willemsen, J.: (1983), *J. Phys. A* **16**, 3365.

Zaitsev, S.: (1992), *Physica A* **189**, 411.